

Field Phenotyping: affordable solutions



The Italian plant phenotyping landscape and the other international initiatives

5 - 6 September 2018, Metaponto - Matera

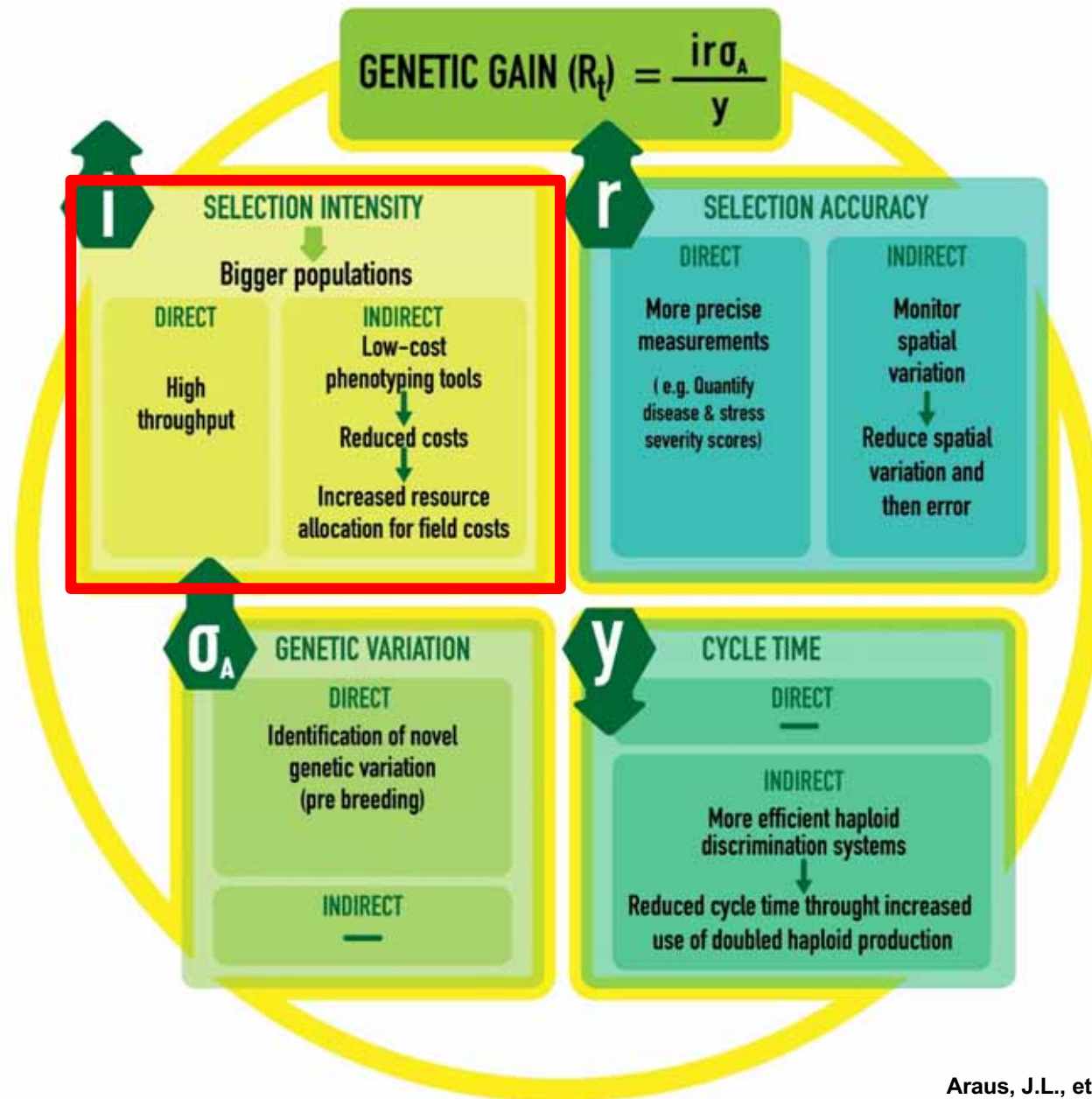
José Luis Araus

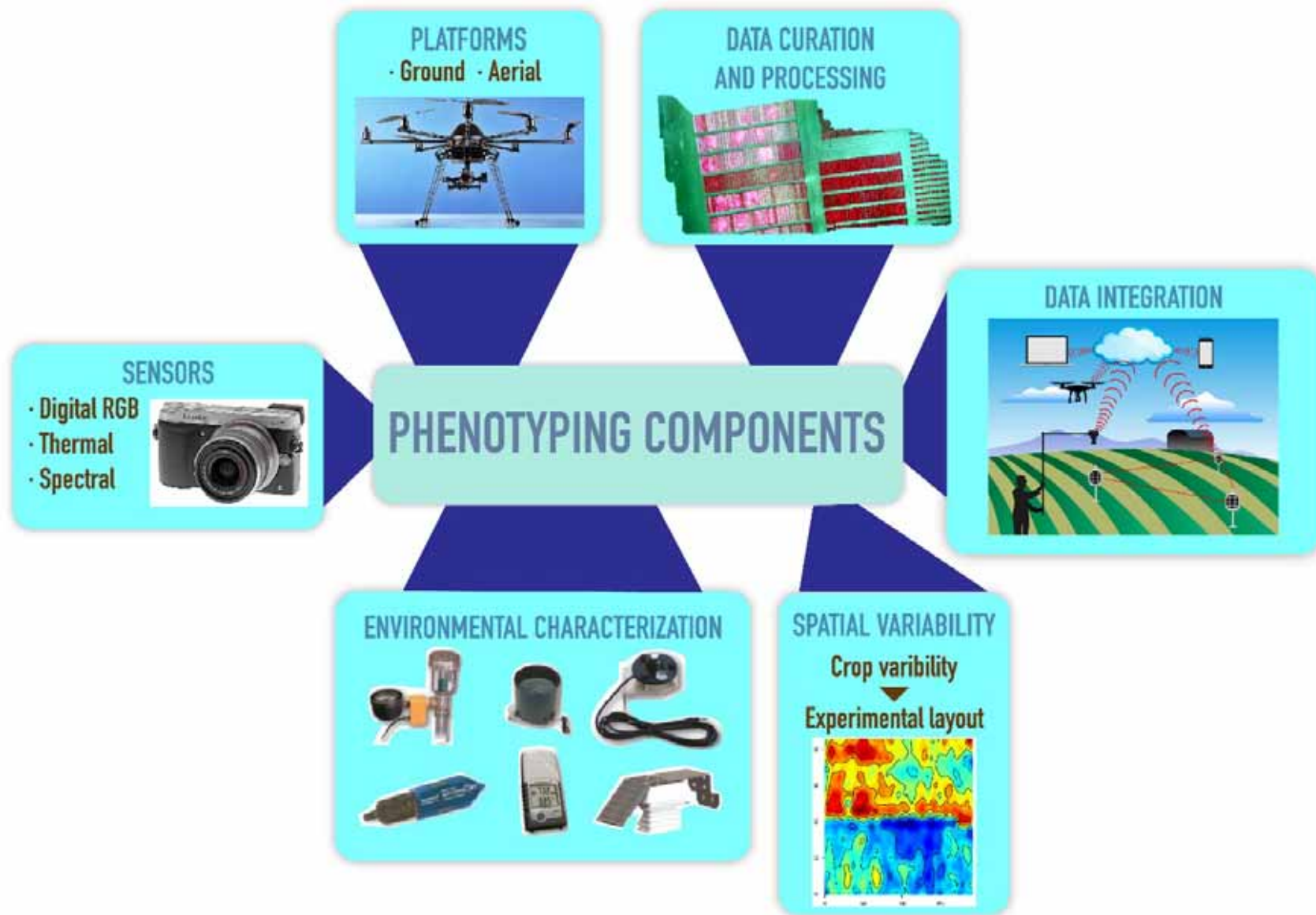


Why affordable?

- The required tools and resources for phenotyping will need to become universal, and the most realistic way to achieve that is through low-cost, open-source technology
- As more researchers have access to the tools and can test and evaluate them within the context of their respective research programs, this will determine if expenditure on these resources was warranted.

Why affordable?





Outline

Affordable Phenotyping

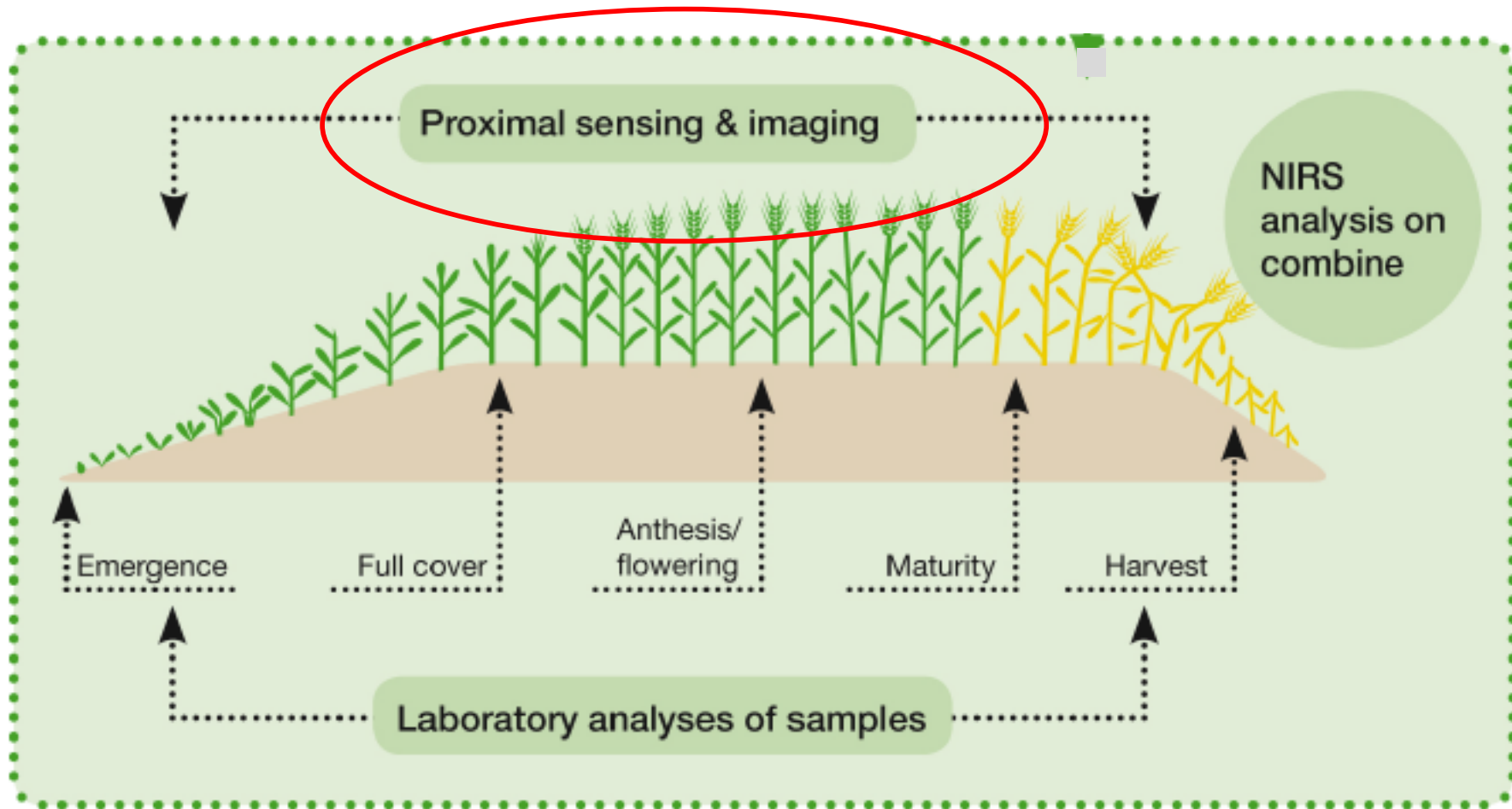
- Sensors
- Platforms
- Environmental characterization
- Data curation and processing
- Data integration

Outline

Affordable Phenotyping

- Sensors
- Platforms
- Environmental characterization
- Data curation and processing
- Data integration

Different categories of sensors



Canopy senescence – visual score

Measurement:

- score from 0-10, divide the % of estimated total leaf area that is dead by 10
- initiation & rate of canopy senescence



1 (10%)



3 (30%)



5 (50%)

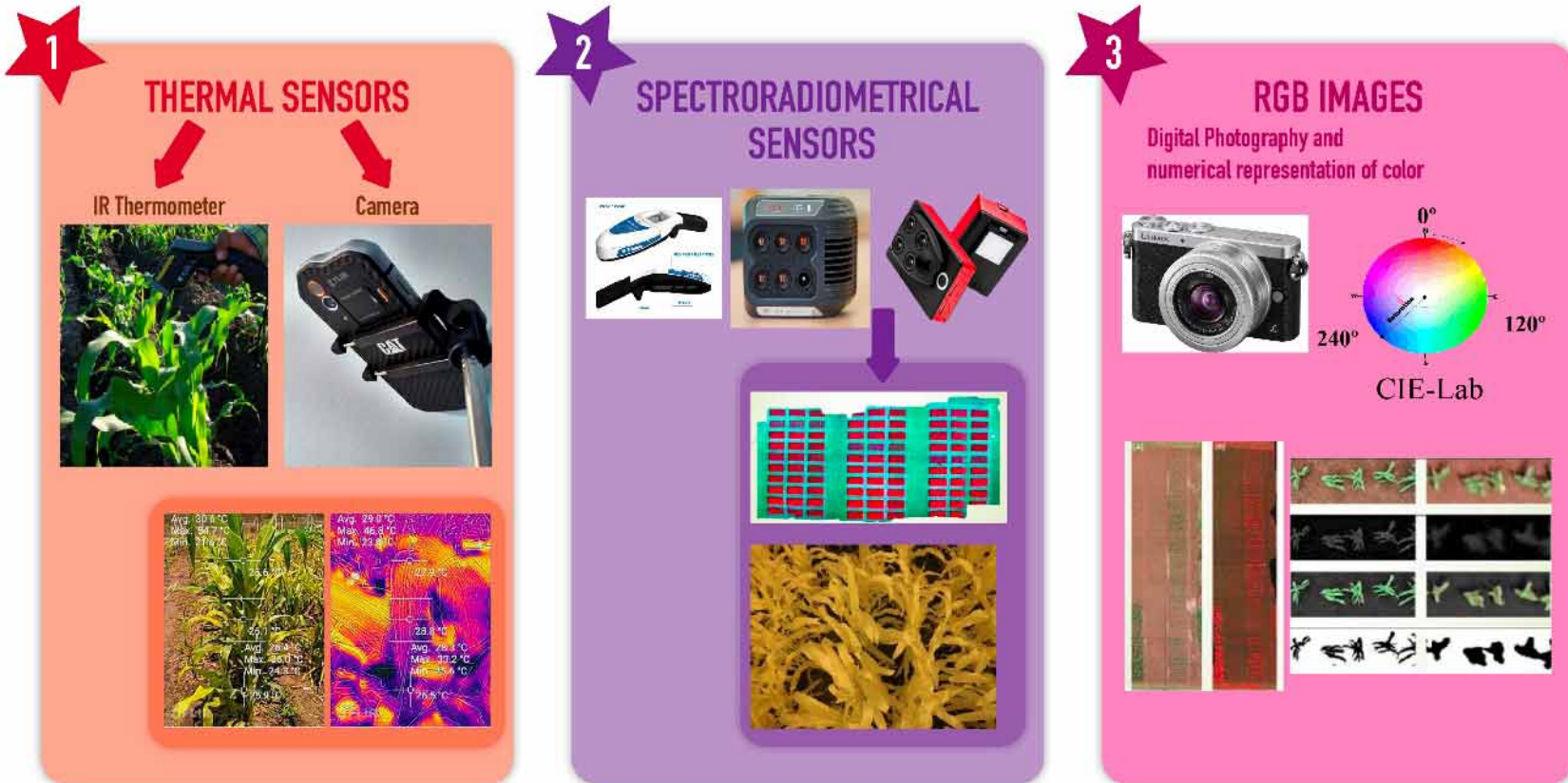


7 (70%)



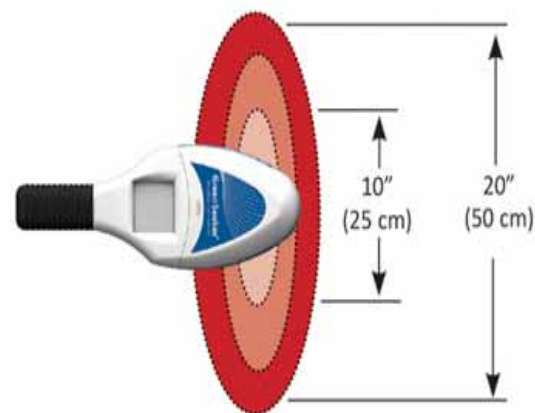
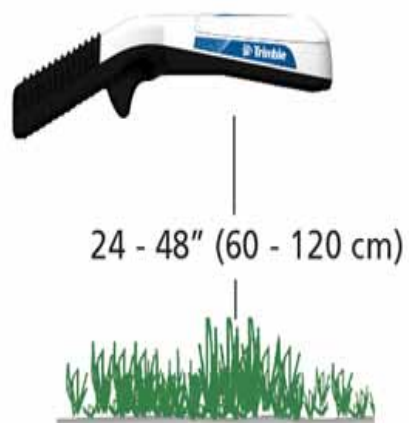
9 (90%)


TYPES OF LOW COST SENSORS



Spectroradiometrical sensors

New!
GreenSeeker®
HANDHELD CROP SENSOR





Other multispectral sensors available with 4-6 sensors (at 500-1000 USD per sensor band)

- ▶ Tetracam 4 band ADC, ADC lite, and microMCA 4 or 6, customizable filters from 400-1000 nm, with or without ILS, optional thermal camera integration, and GPS units available separately.
- ▶ HiPhen AirPhen 6 sensor customizable bandwidth filters multispectral sensor with GPS and optional thermal camera integration.
- ▶ AIRINOV Multispec 4C NDVI-NDRE and NDVI-PRI 4 band sensors with GPS and ILS sensors integrated
- ▶ Parrot Sequoia 4 band + RGB sensor with integrate ILS, GPS and IMU



multiSPEC4c
AIRNOV



MultispeQ v2.0

The MultispeQ combines the functionality of a handheld fluorometer, a chlorophyll meter, and a bench-top spectrometer into one low cost, modifiable tool that brings lab quality measurements to field applications. Measure photosynthetic phenotypes in real field conditions, identify biotic and abiotic stresses in plants or algae, and collect thousands of data points around the world using collaborators in the PhotosynQ network. The MultispeQ is what you wanted all your other tools to be - affordable, powerful, modifiable, and collaborative by design.



PhotosynQ

<https://photosynq.org/>



Software

The PhotosynQ mobile and desktop apps allow users to collect high throughput phenotyping data in the field and connect that data to our sophisticated data explorer. Use the data explorer to view, map, analyze and share collaborative research data quickly and easily.

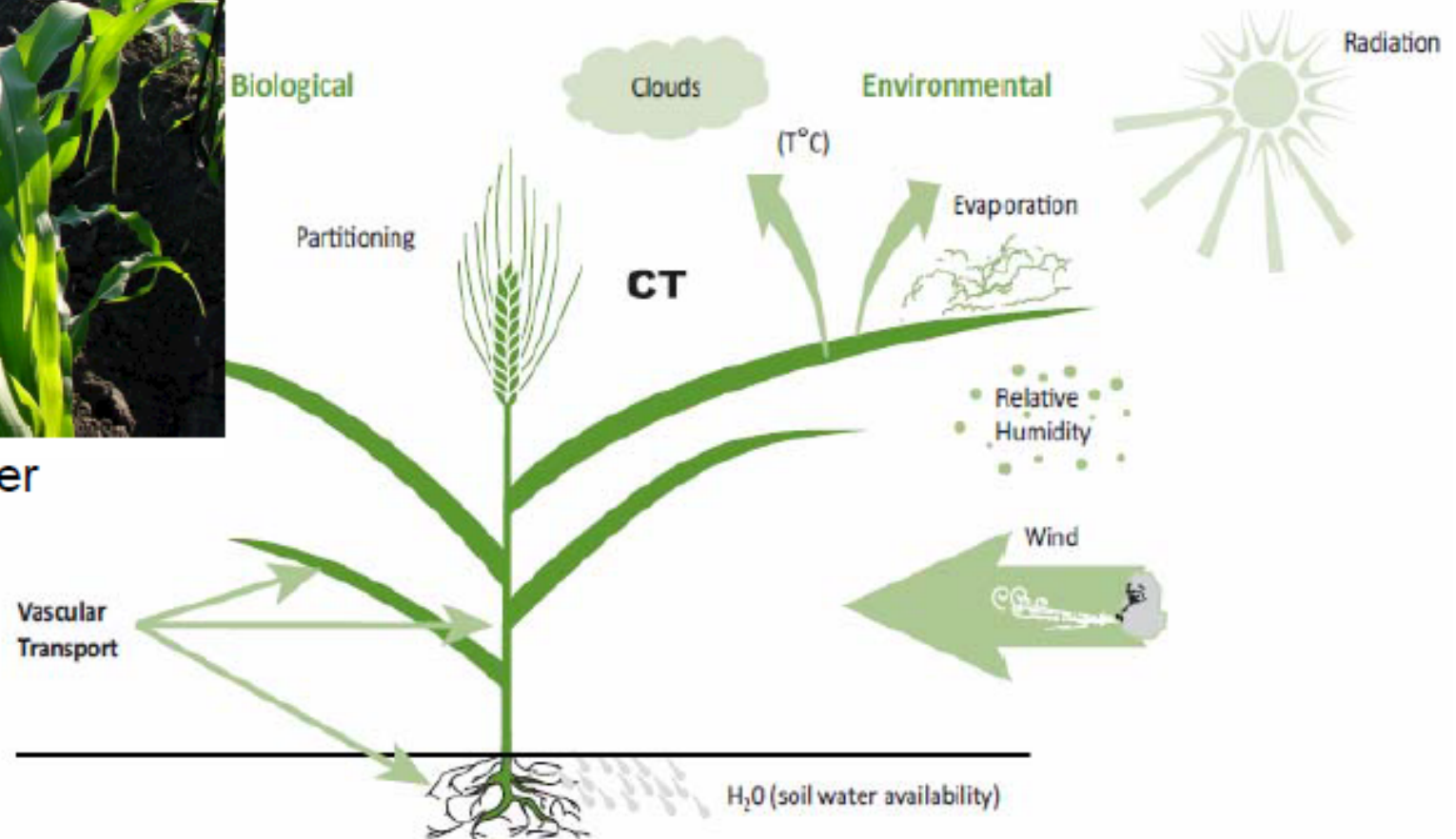
Thermal sensors

Transpiration as a cooling system: IR thermometry



IR Thermometer

With quiet air (i.e. limited air-cooling), differences of several degrees in fully irradiated leaves with changes in stomatal conductance

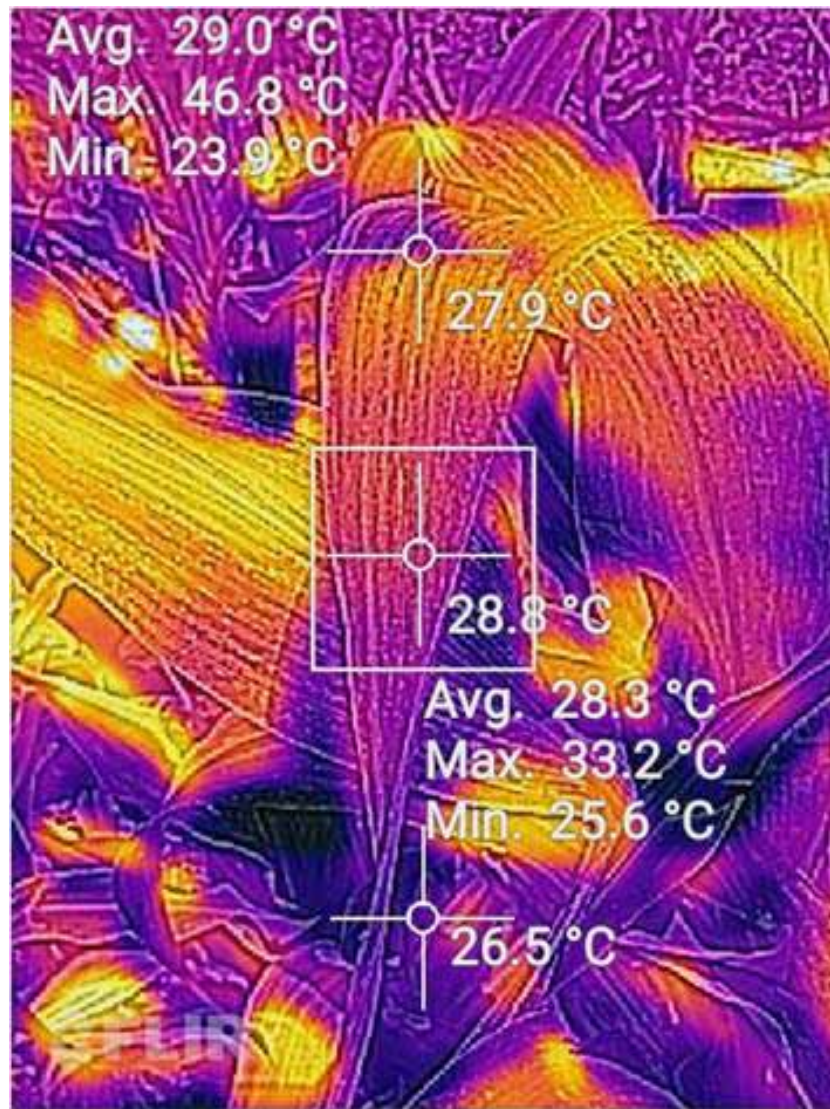
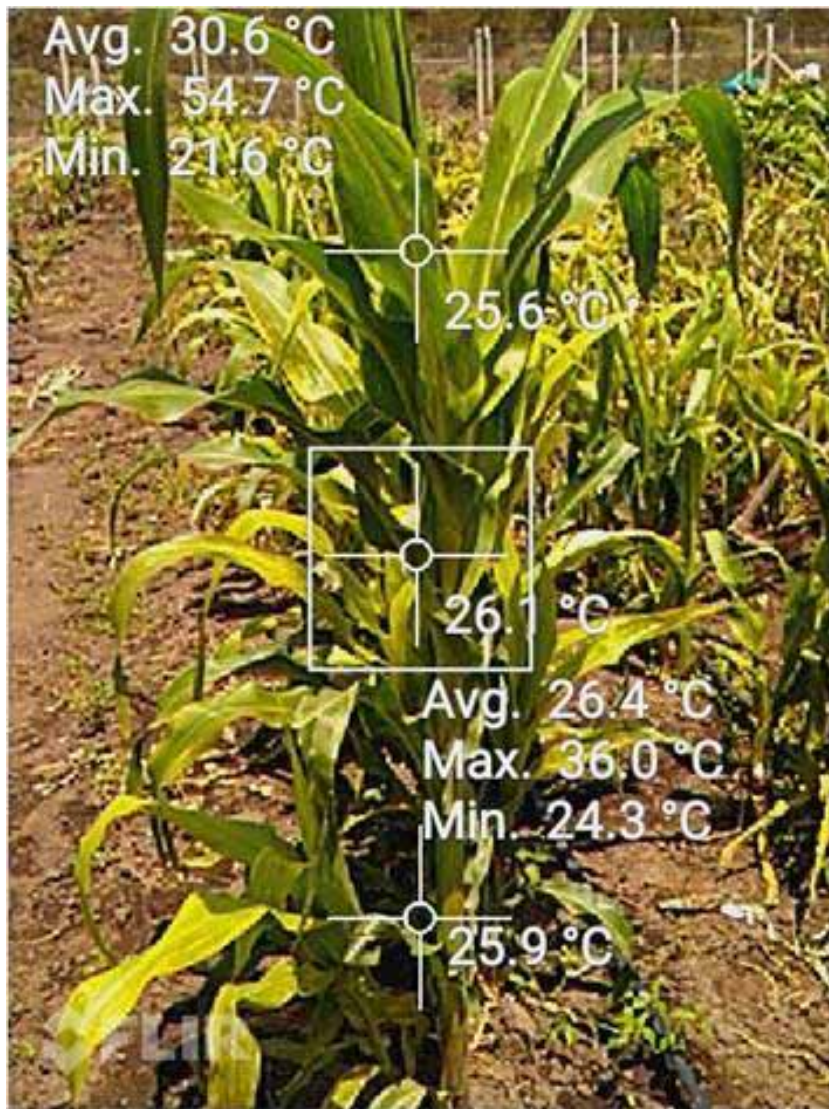


Reynolds, Pask & Mullan 2012

Figure 6.1. Biological (physiological) and environmental factors affecting canopy temperature (Adapted from Reynolds *et al.*, 2001).



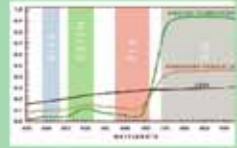
Pictures taken from the camera using the thermal plus RGB fusion, thermal temp point measurements over RGB, and plain thermal camera modes



RGB cameras

RGB Images

Data process -> Open Source Software -> Mobile Apps



<https://github.com/sckefauver/CIMMYT>



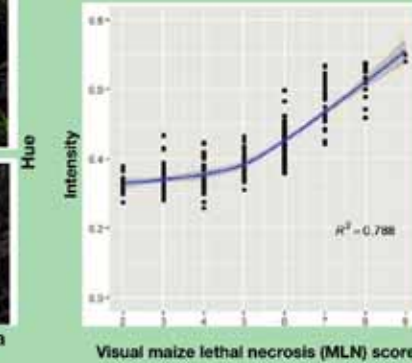
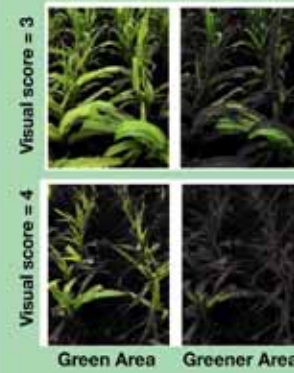
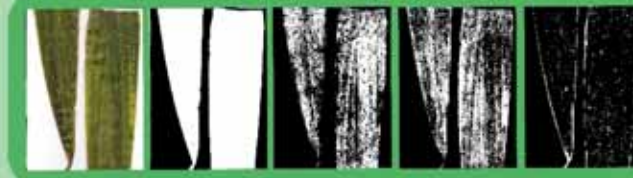
Nitrogen Fertilization

Ground Aerial

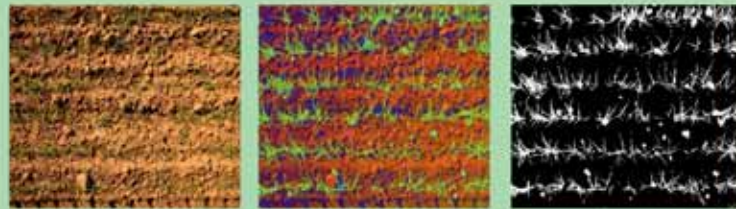


Disease Monitoring

Maize MLN



Seedling Counting / Early Vigor

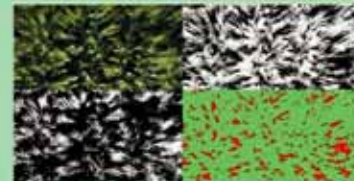


3D Reconstruction

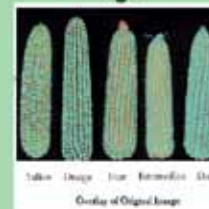


In field Evaluation of Yield Components

Spike Density

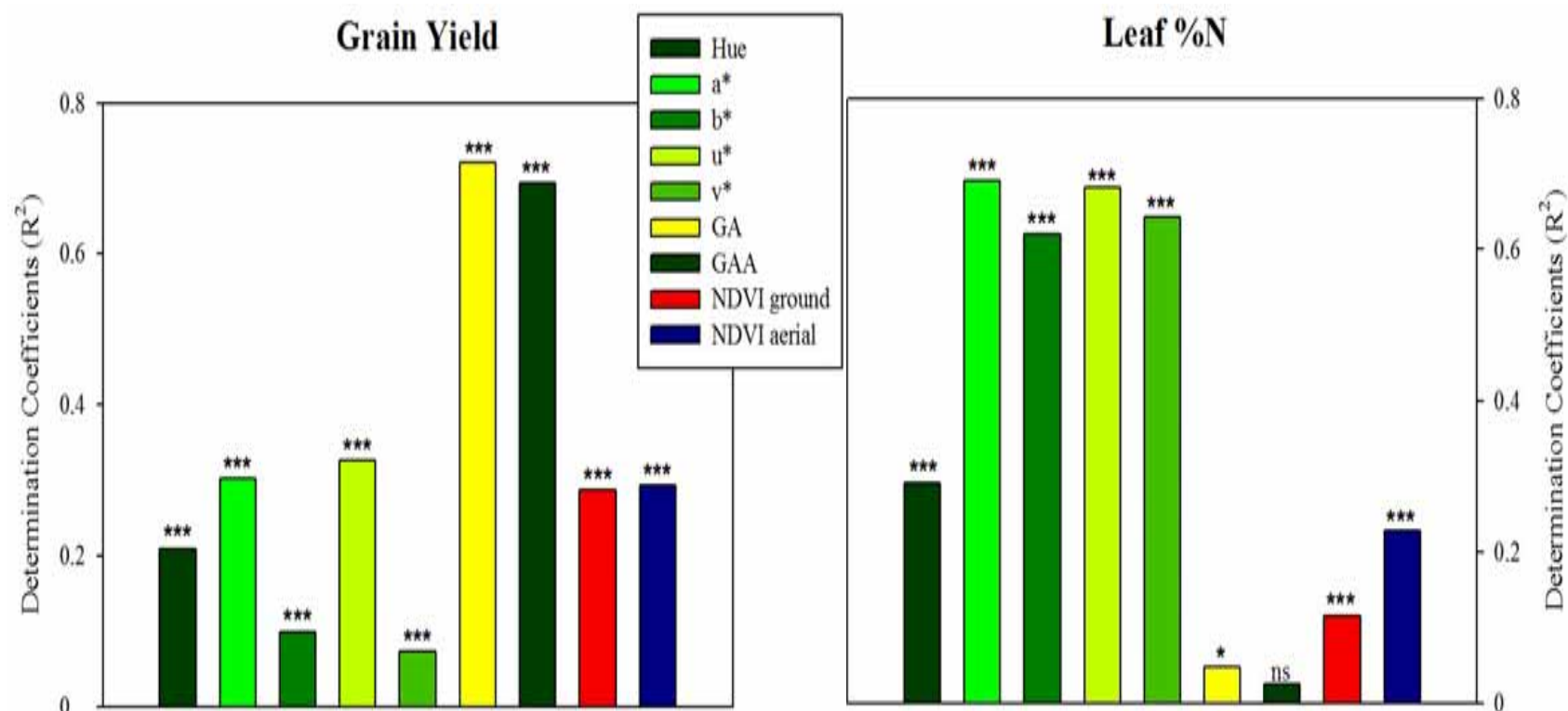


Number of Kernels



RGB vs Spectral indices

N fertilization treatments in maize



Vegetation Indexes

***, $P < 0.001$; **, $P < 0.01$; *, $P < 0.05$; ns, not significant

Wheat – yellow rust

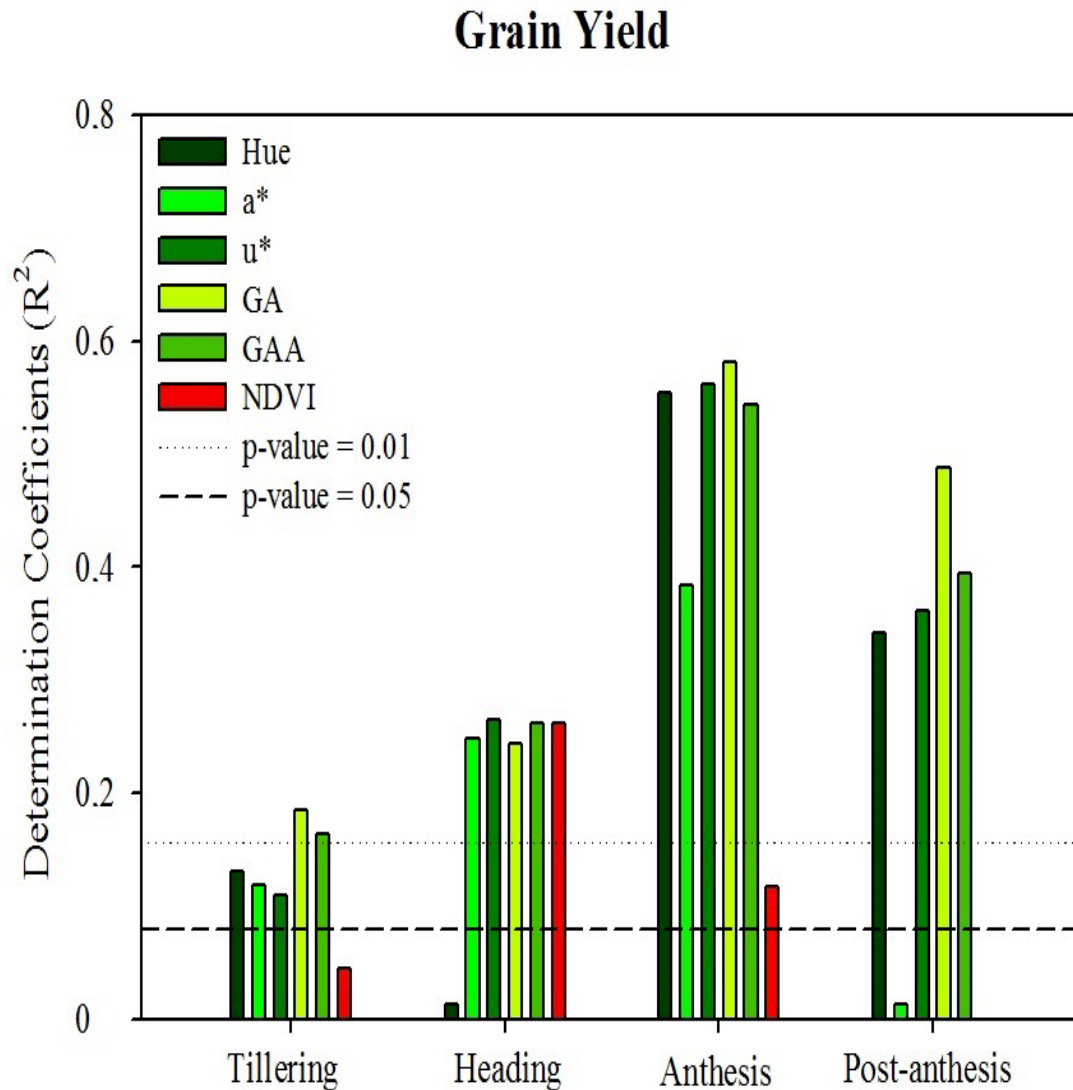


Fig. 1 – Wheat leaves damaged by yellow rust during 2012–2013.

Available online at www.elsevier.com/locate/ces

ScienceDirect

Grain yield losses in yellow-rusted durum wheat estimated using digital and conventional parameters under field conditions

Omar Vergara Diaz^a, Shaim C. Kefauver^a, Abdelhalim Elazab^b, Maria Teresa Nieto-Yaladri^a, José Luis Arauz^a

^aUnit of Plant Pathology, Department of Plant Biology, Faculty of Biology, University of Barcelona, Diagonal 151, 08028 Barcelona, Spain
^bNational Institute for Agricultural and Food Research and Technology (INIA), CITA & La Granja 17, 50003, Madrid, Spain

Computers and Electronics in Agriculture

journal homepage: www.elsevier.com/locate/ces

Low-cost assessment of wheat resistance to yellow rust through conventional RGB images

B. Zhou, A. Elazab, J. Ber, O. Vergara MD, Semt, J.L. Arauz^{*}

^{*} José L. Arauz, Instituto de Investigación en Recursos Cinegéticos, IREC (CSIC-URV), Ronda de Toledo s/n, 13005, Ciudad Real, Spain

Canopy cover and senescence

Table 2. Broad-sense heritability (H^2) and mean of canopy senescence and its genetic correlation with grain yield in three maize hybrid trials (composed of 50 varieties each) evaluated under low soil nitrogen at Harare, Zimbabwe. (Data are means of 450 plots).

	Aerial Imaging	Visual Assessment		
	Sen. Index	Sen1	Sen2	Sen3
Heritability	0.529	0.285	0.585	0.500
Mean	0.466	12.731	28.666	61.944
Genetic correlation with yield	-0.397 **	-0.179	0.006	-0.101
n Replicates	3	3	3	3

** = $p < 0.01$, Sen. = canopy senescence. Sen. index (aerial imaging) corresponds to Sen3 (visual assessment).

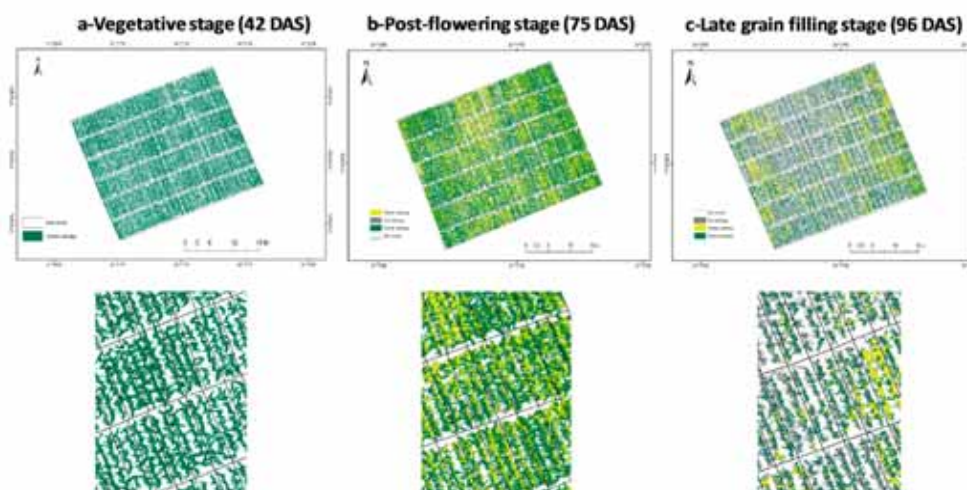


Figure 4. Time sequence aerial images of maize hybrids at three different developmental stages grown at the International Maize and Wheat Improvement Center (CIMMYT)-Harare research station in Zimbabwe. The trials were composed of 50 varieties each, planted using an alpha lattice design with three replicates. (DAS = days after sowing).

RGB images: plant shape

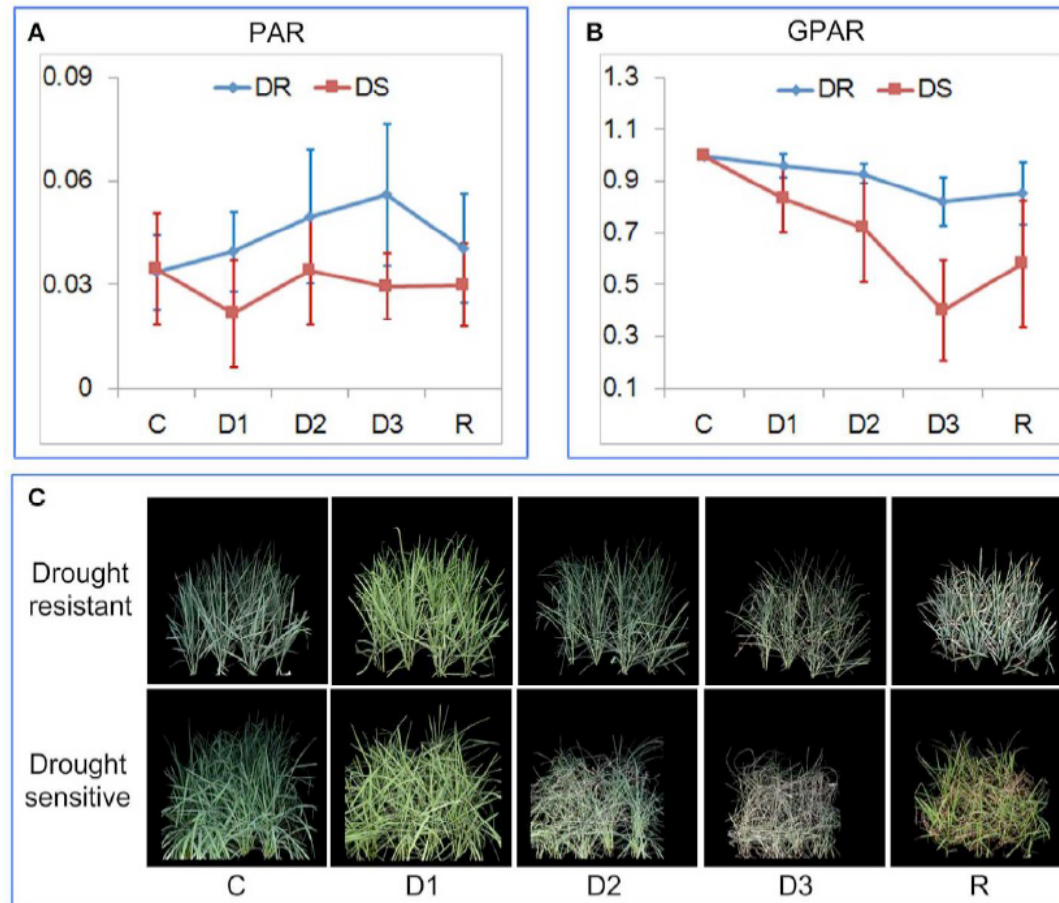


FIGURE 7 | Quantification of rice drought response under field conditions. **(A)** Dynamics of PAR at five time points. **(B)** Dynamics of GPAR at five time points. The markers and the bars in each line represent the mean value and standard deviation across the accessions, respectively. **(C)** A drought resistant accession and a drought sensitive accession at five time points. C, before stress; D1, mild drought stress; D2, moderate drought stress; D3, severe drought stress, and R: after rehydration.



Novel Digital Features Discriminate Between Drought Resistant and Drought Sensitive Rice Under Controlled and Field Conditions

Lingling Duan¹, Jieun Han¹, Zhong Sun¹, Heiko Fu¹, Peng Peng¹, Dong Zhang¹, Xian Fan¹, Guozhong Chen¹, Leihong Xiang¹, Mingqin Dai¹, Kevin Williams¹, Frank Corke¹, John A. Dolan¹ and Wanning Yang^{1*}

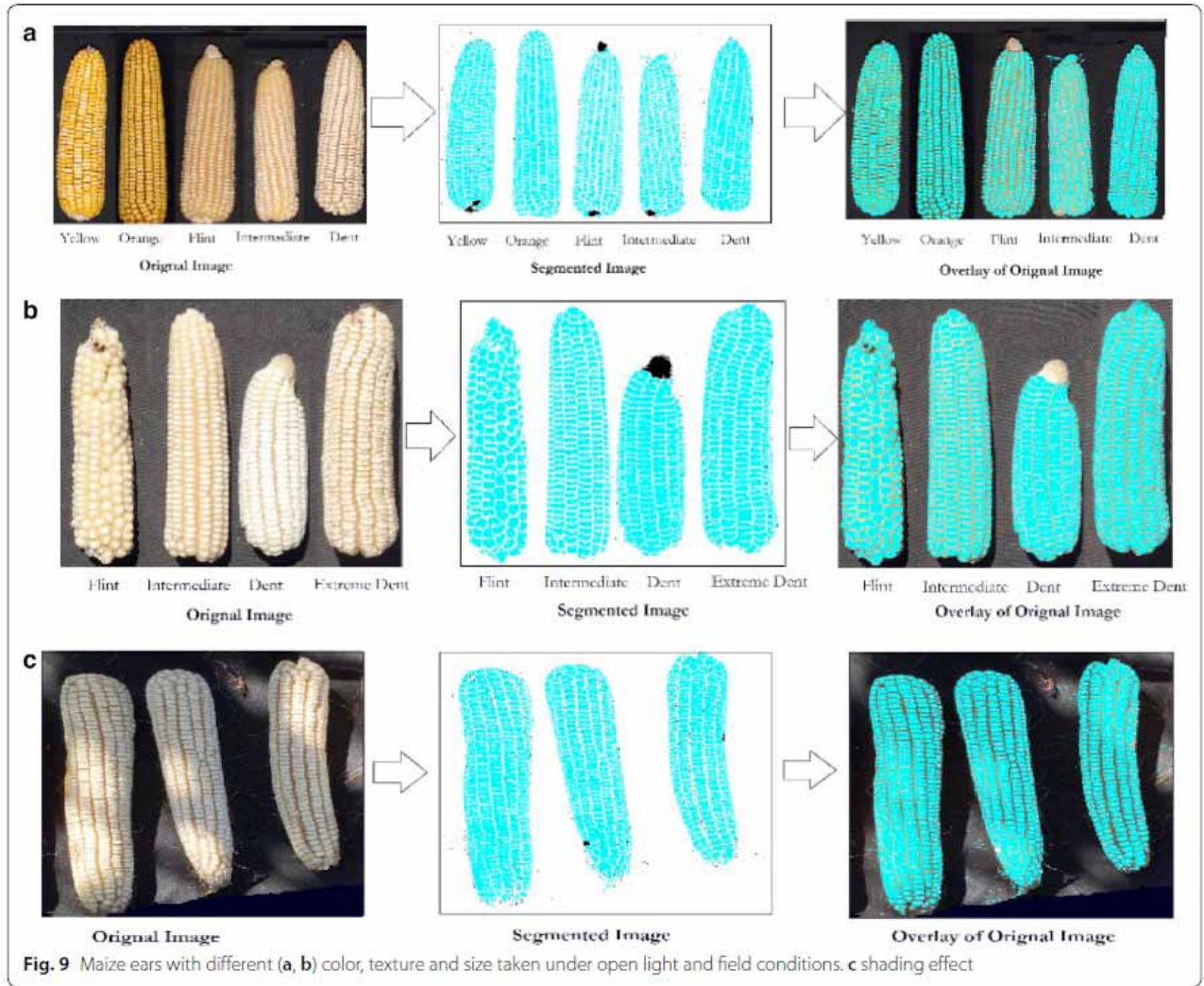
RGB images: plant height

Table 3 Performance comparison of each sensing technique

Sensors	Carriers	Performance			
		Resolution	Equipment cost per unit	Accuracy compared with the ground truth	Data processing cost
LIDAR-Lite v2 sensor	Ground vehicle	Low, only reflect	< \$100	Low, due to the low sampling frequency	Low
Ultrasonic sensor		1-dimensional measurements	\$300–\$800	High	
Kinect camera	UAV	~0.2 MP	< \$300	High, within the optimal measuring range	High, due to photogrammetry processing
DSLR cameras		~18 MP	> \$800	Highest	
Digital cameras		~12 MP	< \$600	r = 0.73	



RGB images: ear characteristics



Malvar et al. *Plant Methods* (2012) 10:49
<https://doi.org/10.1186/1745-2758-10-49>

Plant Methods

METHODOLOGY

Open Access

High-throughput method for ear phenotyping and kernel weight estimation in maize using ear digital imaging



RGB images: ear characteristics

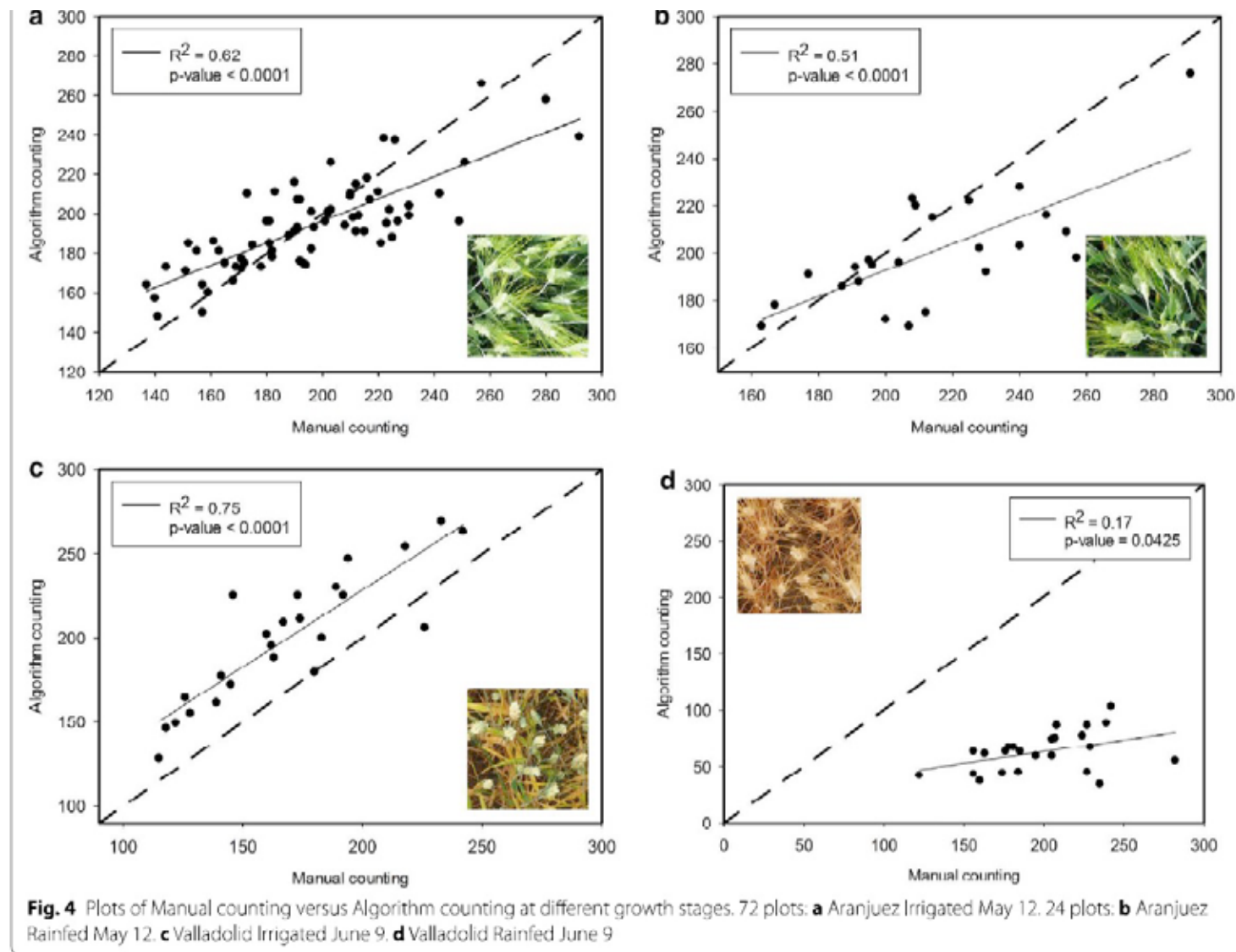
Table 2 Broad-sense heritabilities (H^2) and means for grain yield and kernel/ear attributes estimated through imaging for six maize trials with three replicates evaluated under low soil nitrogen at Harare, Zimbabwe

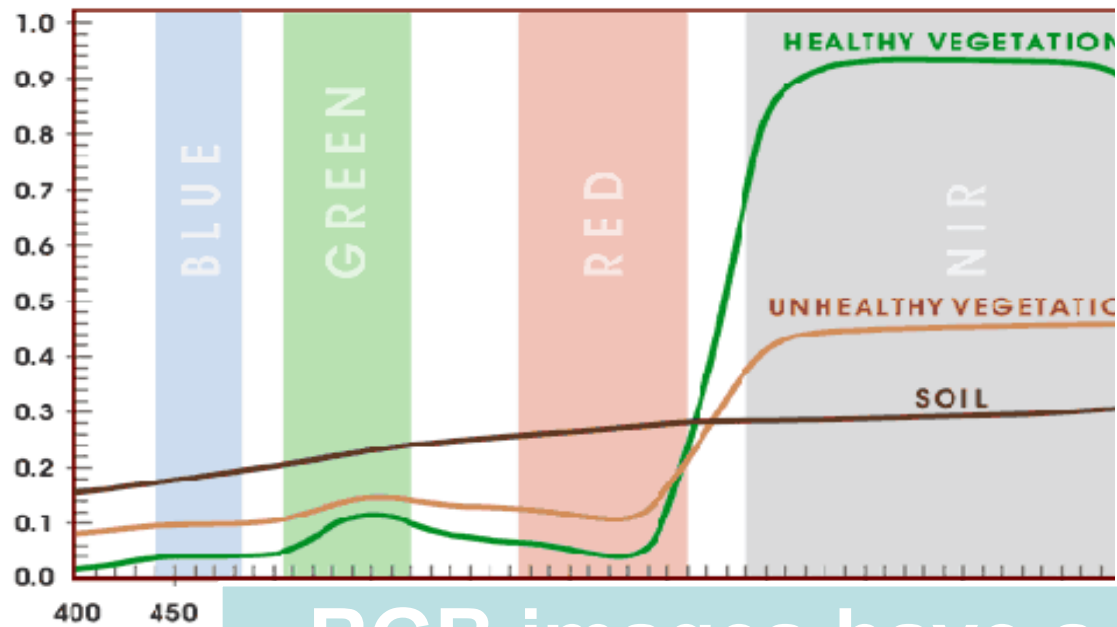
Trial	Number of		Measured Grain yield(Mg ha ⁻¹)	Broad-sense heritability (H^2)										
	Entries (hybrids)	Year		Kernel attributes							Ear attributes			
				Visible Kernel Number	Mean width (cm)	Mean length (cm)	Total area (cm ²)	Mean area (cm)	Mean perimeter (cm)	Total Number per plot	Total Weight (g plot ⁻¹)	Number per plot	Mean length (cm)	Mean width (cm)
EHYB1746	50	2017	0.591	0.374	0.725	0.815	0.439	0.71	0.842	0.374	0.301	0.781	0.665	0.507
EHYB1747	50	2017	0.596	0.619	0.657	0.761	0.513	0.722	0.765	0.619	0.492	0.358	0.728	0.634
EHYB1748	50	2017	0.595	0.624	0.709	0.624	0.687	0.69	0.569	0.597	0.700	0.746	0.539	0.278
IHYB1747	50	2017	0.599	0.721	0.737	0.693	0.423	0.607	0.735	0.721	0.442	0.515	0.652	0.504
LHYB1619	55	2016	0.146	0.541	0.904	0.930	0.238	0.917	0.934	0.541	0.320	0.647	0.560	0.730
LHYB1617	55	2016	0.137	0.314	0.798	0.830	0.384	0.782	0.903	0.314	0.287	0.450	0.279	0.239
Mean			0.444	0.532	0.755	0.775	0.447	0.738	0.769	0.527	0.423	0.582	0.570	0.482
				Mean										
EHYB1746	50	2017	4.02	4510.01	0.36	0.66	760.64	0.17	1.85	9243.27	3001.43	24.51	14.95	4.81
EHYB1747	50	2017	5.48	5337.80	0.35	0.65	858.42	0.16	1.81	10941.06	3452.16	28.22	14.71	4.70
EHYB1748	50	2017	2.60	4781.87	0.36	0.67	801.47	0.14	1.91	9800.89	3237.06	27.88	14.42	4.66
IHYB1747	50	2017	5.20	5398.55	0.34	0.63	824.45	0.15	1.77	11065.71	3318.40	28.05	14.34	4.64
LHYB1619	55	2016	2.24	3789.83	0.42	0.76	852.04	0.23	2.31	7766.21	2415.55	21.77	16.43	5.23
LHYB1617	55	2016	1.36	3151.16	0.35	0.60	435.25	0.14	2.02	4420.99	1126.73	23.18	11.17	3.93

EHYB early hybrid trial, IHYB intermediate hybrid trial, LHYB late hybrid trial



Ear counting





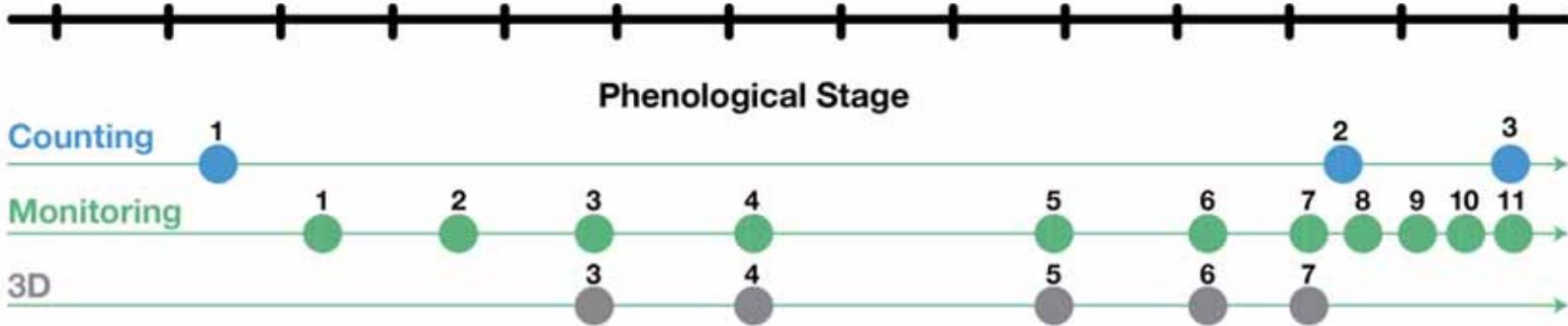
RGB images have a more limited spectral range

but they have an **excellent spatial resolution**

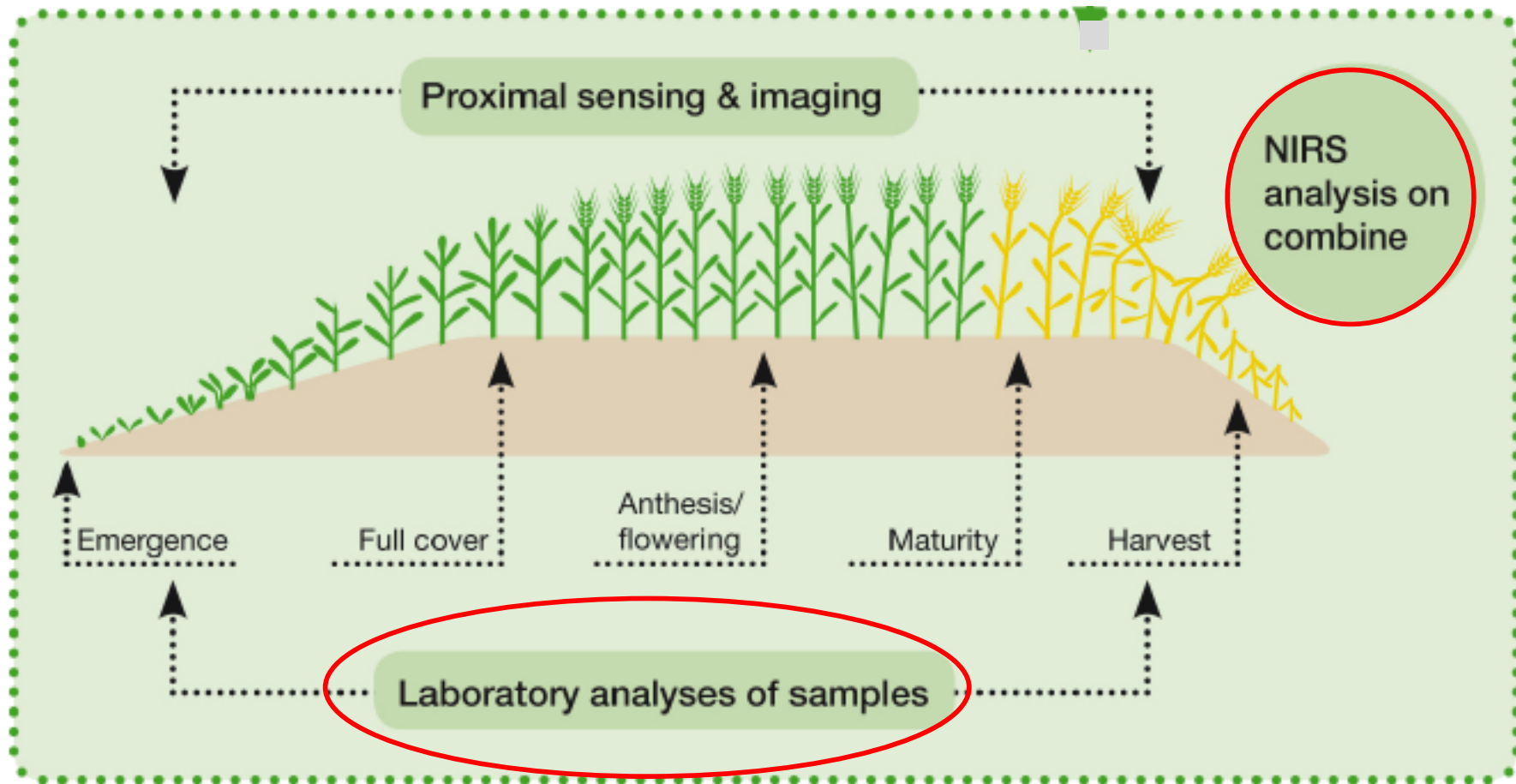
A matter of resolution

- Sometimes high spectral resolution (such as the infrared and thermal images) can be substituted for high spatial resolution with equal results.
- For example, by digital RGB conventional photography, which has a very high spatial resolution (mm).
- Or even better with conventional RGB photography at high temporal resolution (e.g. weekly).

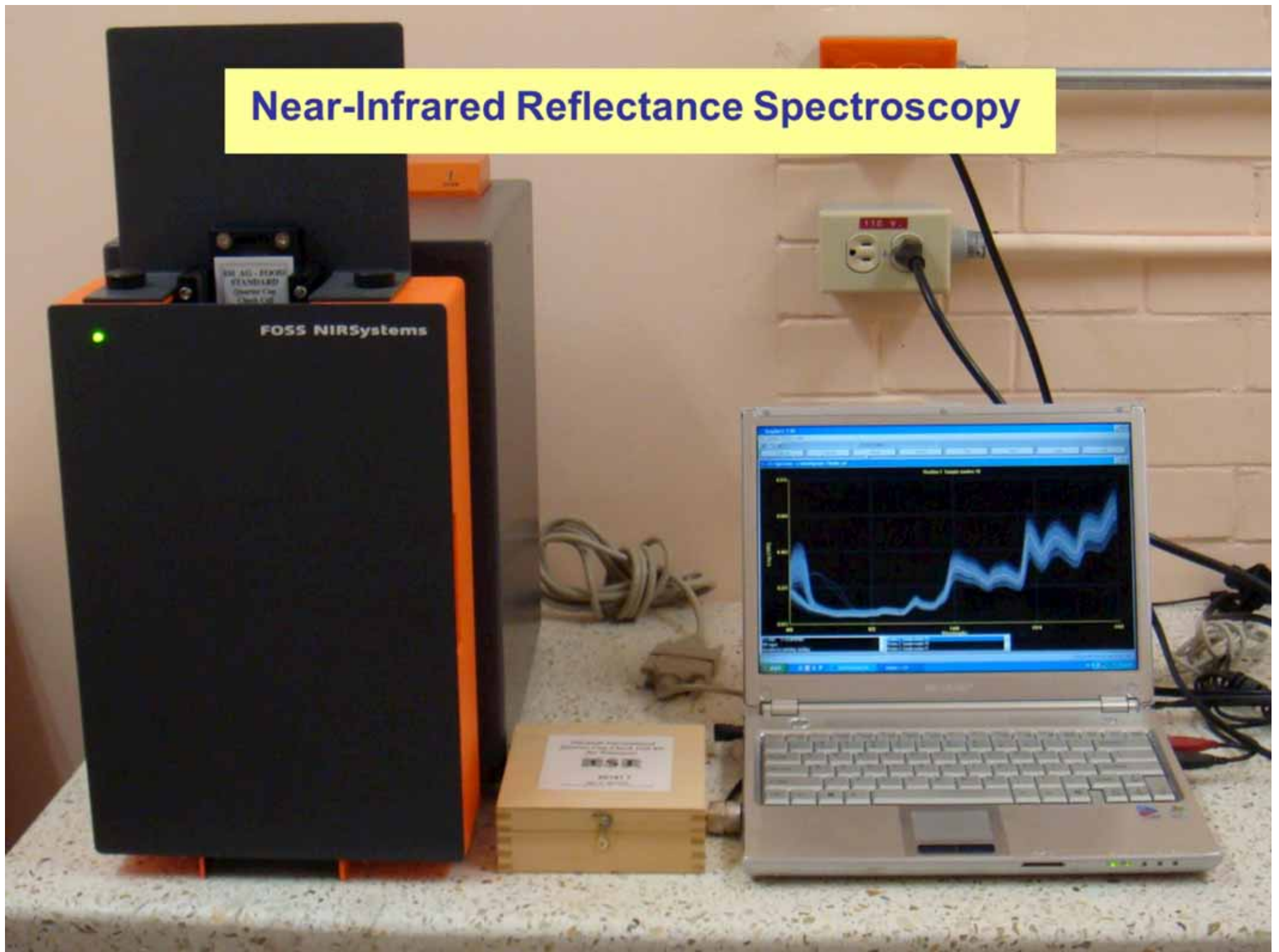
RGB Images



Different categories of sensors



Near-Infrared Reflectance Spectroscopy



Comparative of cost and time

Technique	IRMS		EA	AACC Method	NIRS-prediction			
Parameter	$\delta^{13}\text{C}$	$\delta^{18}\text{O}$	N content	Ash content	$\delta^{13}\text{C}^*$	$\delta^{18}\text{O}$	Ash	N
Cost per sample	10€	20€	3€	1.5€	0.5€			
Time	<10 min	<10 min	<10 min	≈24 h	≈3 min			
Equipment	EA-IRMS		EA	Muffle furnace	NIR spectrometer			



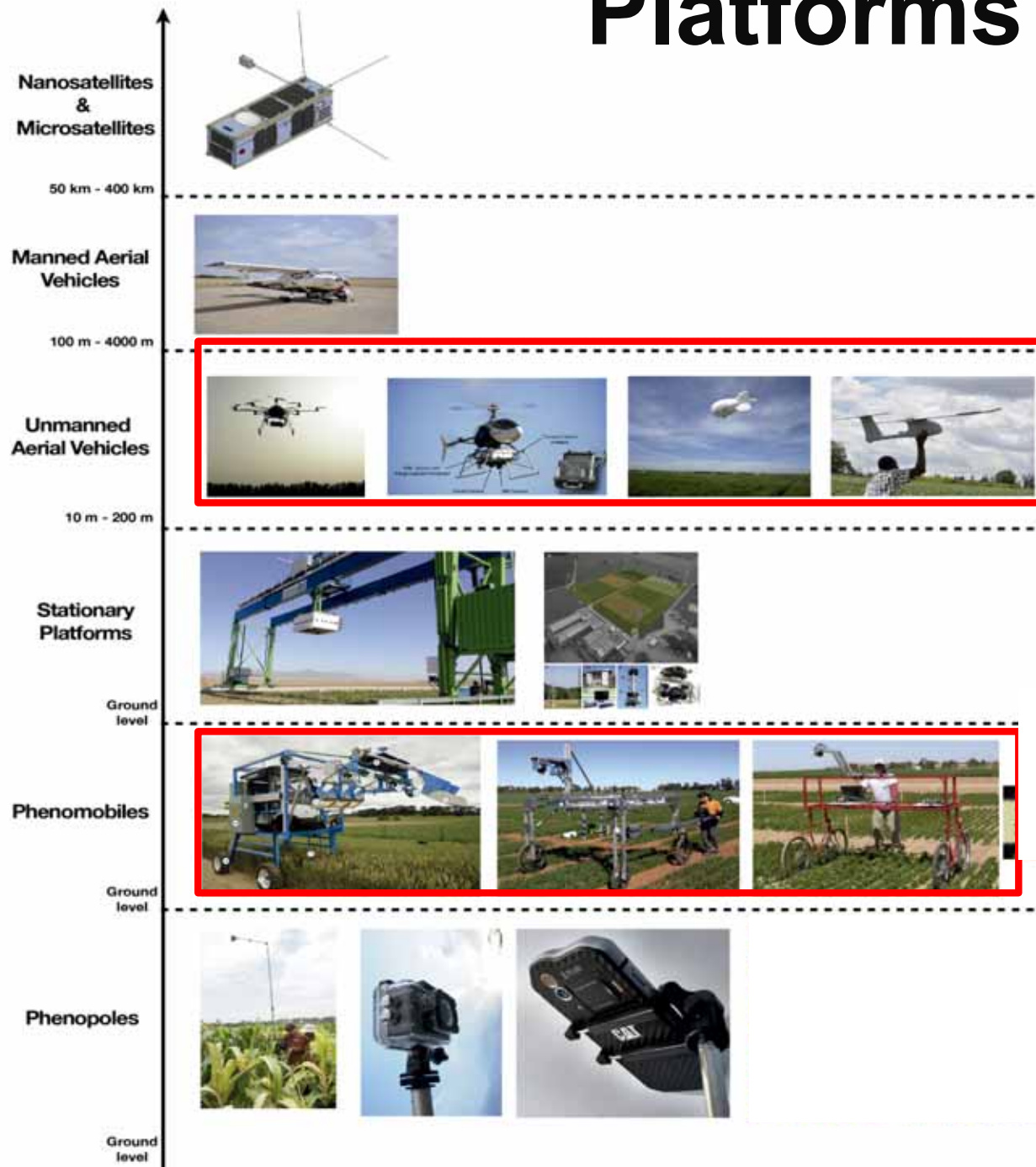
*previously reported by Clark *et al.* 1995; Ferrio *et al.* 2001; Kleinebecker *et al.* 2009

Outline

Affordable Phenotyping

- Sensors
- Platforms
- Environmental characterization
- Data curation and processing
- Data integration

Platforms



Comparative costs

Table 1

Imaging costs involving vehicle, sensors, associated software and personnel in field experiments or in a robotized platform, for two scenarios of demand for phenotyping (offer or demand-limited) and, in the field, three categories of vehicles (vectors) carrying sensors (automated or hand-held ground vehicle or unmanned aerial vehicle (UAV). Costs are expressed in US dollars per plot.day per year (field) or plant.day per year (robotized platform), with the principles of calculations in the panel "vector". Costs of manpower are calculated per year and plot.day or plant.day. Two scenarios are considered for field conditions: in scenario 1 (offer limited), the demand for phenotyping exceeds the capacity of the system; in scenario 2 (demand limited) the demand represents a maximum of 4000 microplots per year.

	Hypotheses for each scenario	Days of use year ⁻¹	Throughput, μ plot or plant day ⁻¹	Vector			Sensors Equivalent calculation, 4 year life	Manpower + training		Maintenance \$ year ⁻¹	\$ per plot day.plot per year	Cost imaging \$ per plot day per year
				Expected duration, year	Investment k\$	Investment \$ per plot per day vector life		\$ year ⁻¹	per plot day per year			
High throughput field experiments, 'offer limited'	Limited by availability of equipment and personnel.											
Automated ground vehicle		60	1200	20	430	0.30	0.24	19564	0.2717	15000	0.2083	1.02
Hand-held ground vehicle		50	800	15	50	0.08	0.44	15553	0.3888	3000	0.0750	0.98
UAV		40	4000	2	10	0.03	0.09	24545	0.1534	2000	0.0125	0.29
High throughput field experiments, 'demand limited'	Limited by the demand for microplot per year. 40,000 μ plots year ⁻¹											
Automated ground vehicle		33	1200	20	430	0.54	0.44	12873	0.3218	15000	0.3750	1.67
Hand-held ground vehicle		50	800	15	50	0.08	0.44	15553	0.3888	3000	0.0750	0.98
UAV		10	4000	2	10	0.13	0.38	17018	0.4255	2000	0.0500	0.98
Robotized indoor platform	Limited by availability of equipment and personnel.	270	1700	15	1000	0.15	0.02	103618	0.2257	15000	0.0327	0.42



What is cost-efficient phenotyping? Optimizing costs for different scenarios
 Daniel Reynolds^{1,2}, Frédéric Baret^{1,2}, Claude Welcker^{1,2}, Aaron Barron^{1,2}, Joshua Bell¹,
 Francesco Cellini¹, Argilla Lorenzini¹, Ashish Choudhary¹, Mehdi Khafri¹, Koji Nishida¹,
 Mark Mueller-Landau¹, Ji Zhou^{1,2}, François Tardieu^{1,2}

Affordable platforms



Outline

Affordable Phenotyping

- Sensors
- Platforms
- **Environmental characterization**
- Data curation and processing
- Data integration

Environmental characterization

Figure 1. Components of platform.

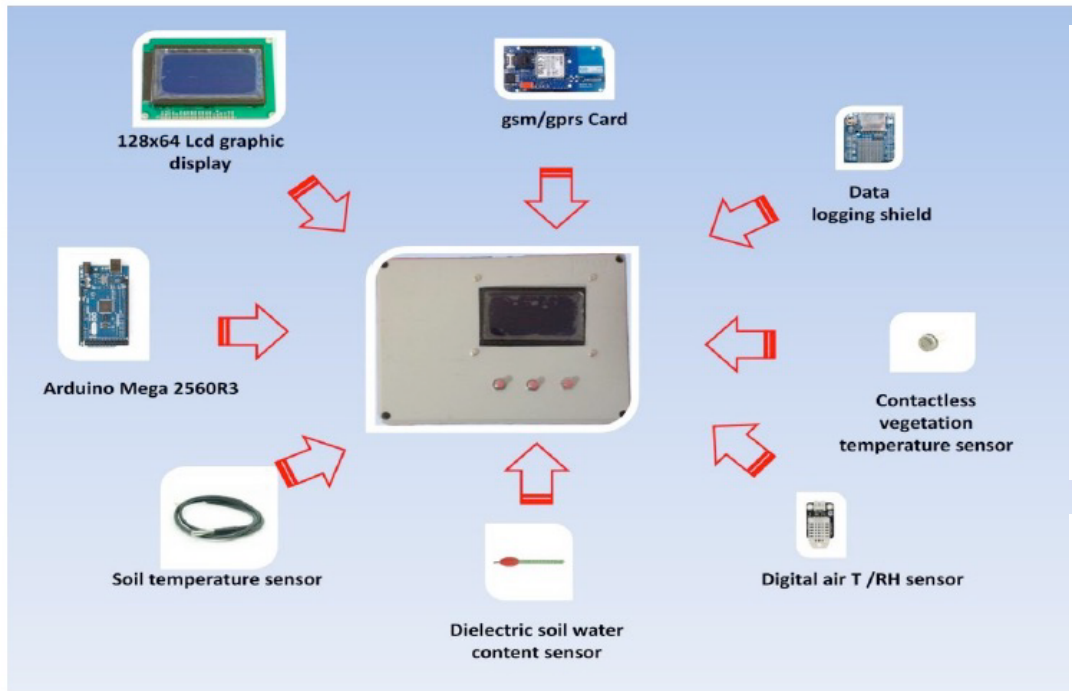


Table 1. Prices of the main components of the platform (source [53]).

Platform Electronic Components	Price in €, Vat Excluded
Adafruit datalogging shield	20
Arduino mega	39
Arduino GSM Shield	69
Optional display	18
DC/DC converter 12 V to 5 V 3 A	5
SD card 2 GB	2
AC 110B-220 V to DC 12 V 3 A regulated transformer power supply	10
Additional electronic materials (connectors, resistors, capacitors)	20
Electronic enclosure	10
Total	193

Figure 2. Platform architecture: (a) schematic representation of a measurement unit; (b) (inset) electronic components inside the indoor enclosure (top-view) and magnification of the micro-controller board and the superimposable expansion shields.

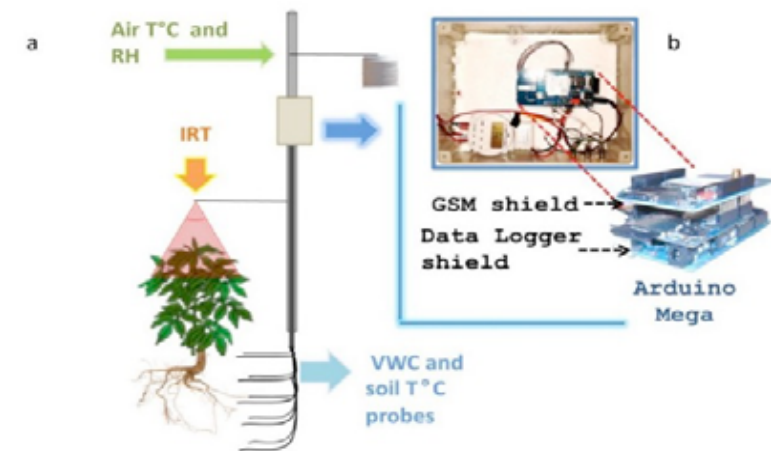
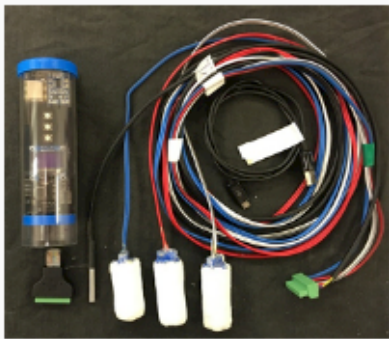


Figure 2. Platform architecture: (a) schematic representation of a measurement unit; (b) (inset) electronic components inside the indoor enclosure (top-view) and magnification of the micro-controller board and the superimposable expansion shields.

Environmental characterization



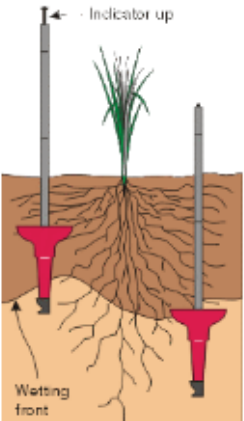
Chameleon Soil Water Sensor

The Chameleon Soil Water Sensor measures how hard it is for plants to suck water out of the soil and the data is displayed as coloured lights.

[More Info](#)



<https://via.farm/>



FullStop Wetting Front Detector

The FullStop Wetting Front Detector tells you how deep water moves into the soil during and shortly after irrigation. It also captures a soil water solution sample which can be extracted using a syringe.



Measuring Nutrients

Nitrate test strips are used to indicate the amount of nitrate moving in the root zone. Nitrate (the main form of soluble nitrogen in soils) moves with water and is easily leached from the soil by over-irrigation.

[More Info](#)



Measuring Salt

Pocket EC meters (Electrical Conductivity) are used to show whether salt is building up in the root-zone (under irrigation) or being continually flushed out (over-irrigation).

[More Info](#)

Outline

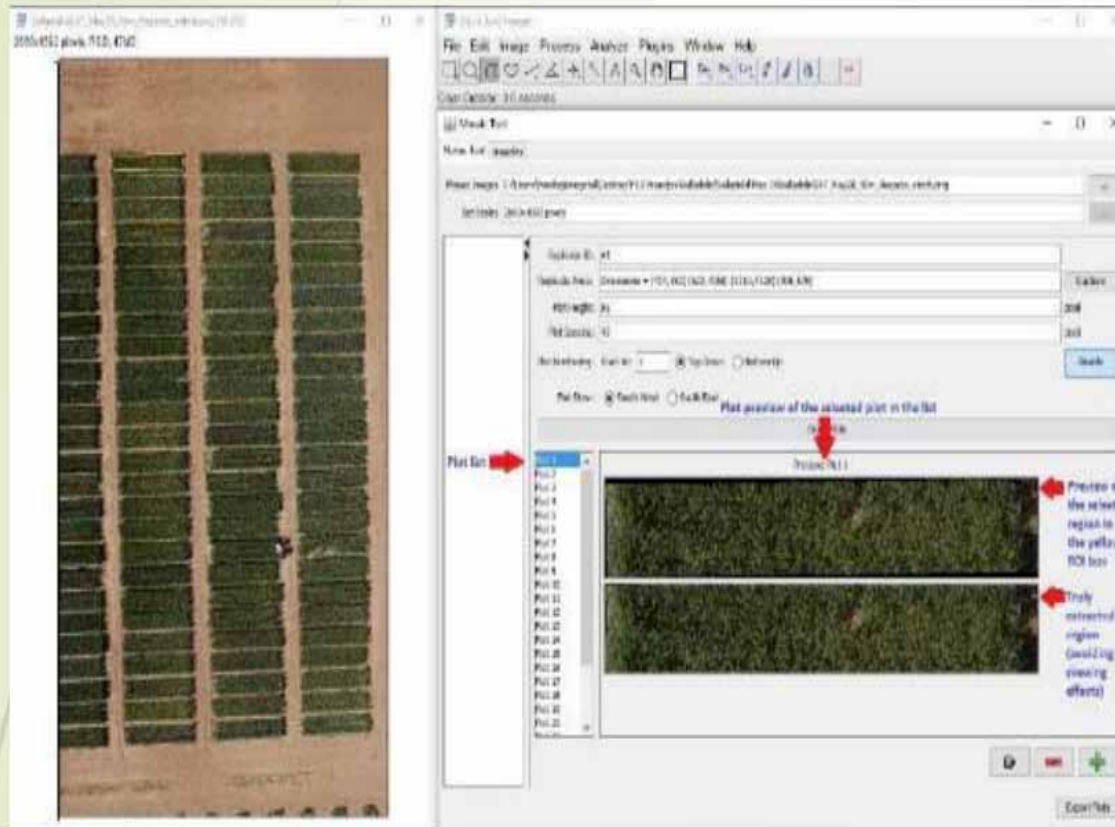
Affordable Phenotyping

- Sensors
- Platforms
- Environmental characterization
- **Data curation and processing**
- Data integration

MosaicTool (Plugin for FIJI)

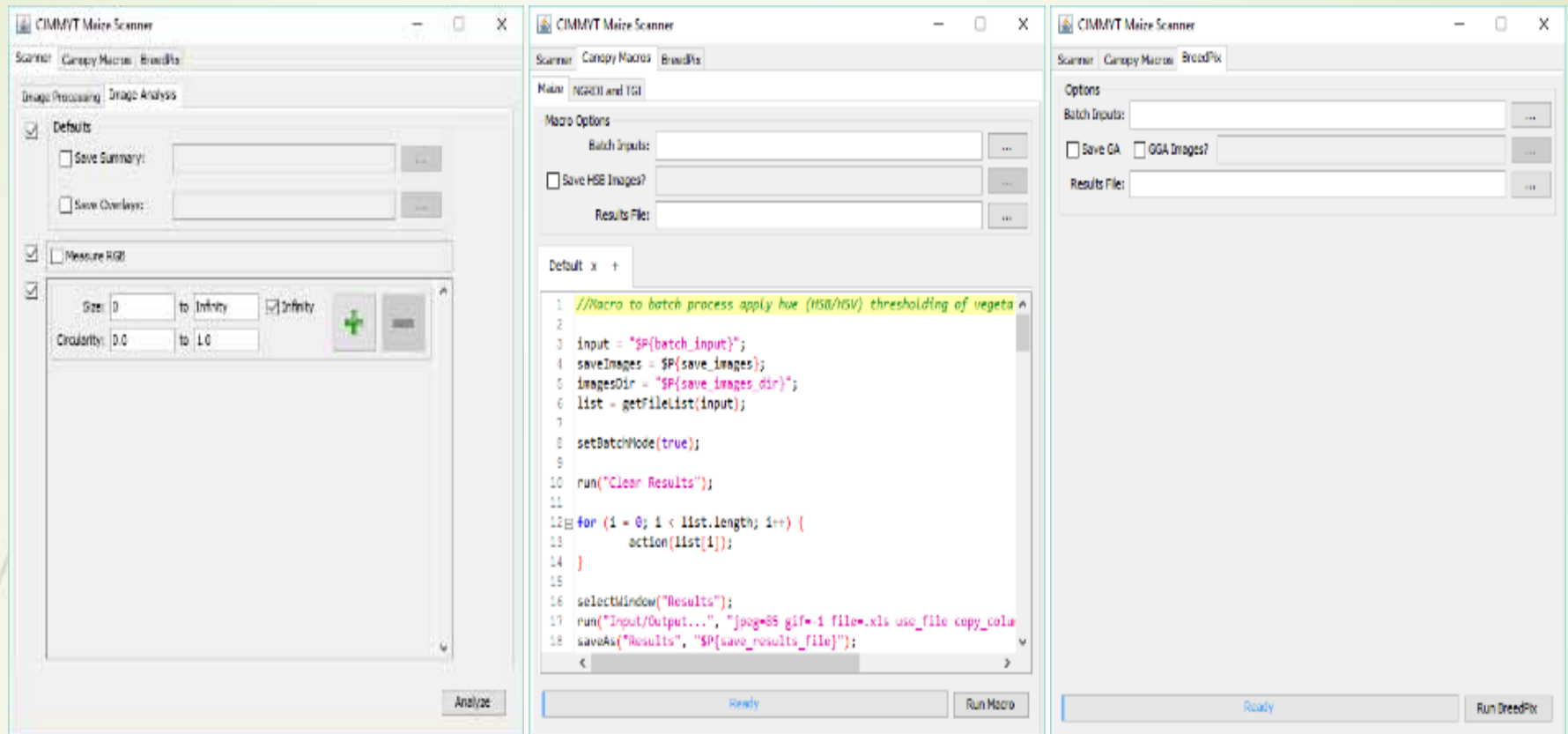
Semi-automatic image segmentation for UAV plant phenotyping studies.

Allows for the extraction and processing of ~1000 plots per hour with quality control









CIMMYT Maize Scanner for RGB field-based phenotyping (released at <http://github.com/george-haddad/CIMMYT>)

Calculates a number of RGB based indexes for estimating disease impacts, crop vigor, LAI, biomass at the leaf and canopy scale, including Breedpix (GA and GGA), Triangle Greenness Index (TGI), and Normalized Green Red Difference Index (NGRDI)

RGB, Green Area, Greener Green Area

MLN plot score 3.0



Maize Leaf Plot RGB



GA (healthy pixels)



GGA (very healthy pixels)

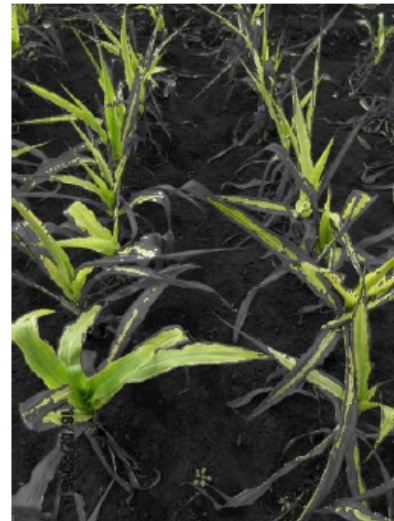


NGRDI (vigor index)

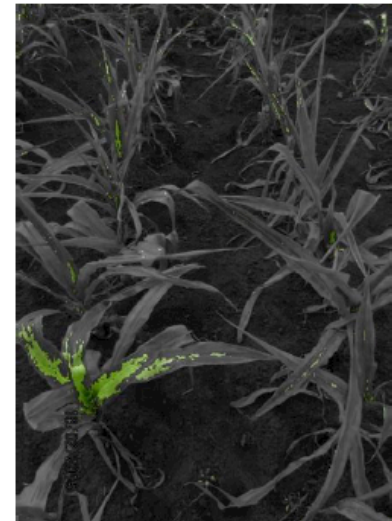
MLN plot score 4.0



Maize Leaf Plot RGB



GA (healthy pixels)



GGA (very healthy pixels)

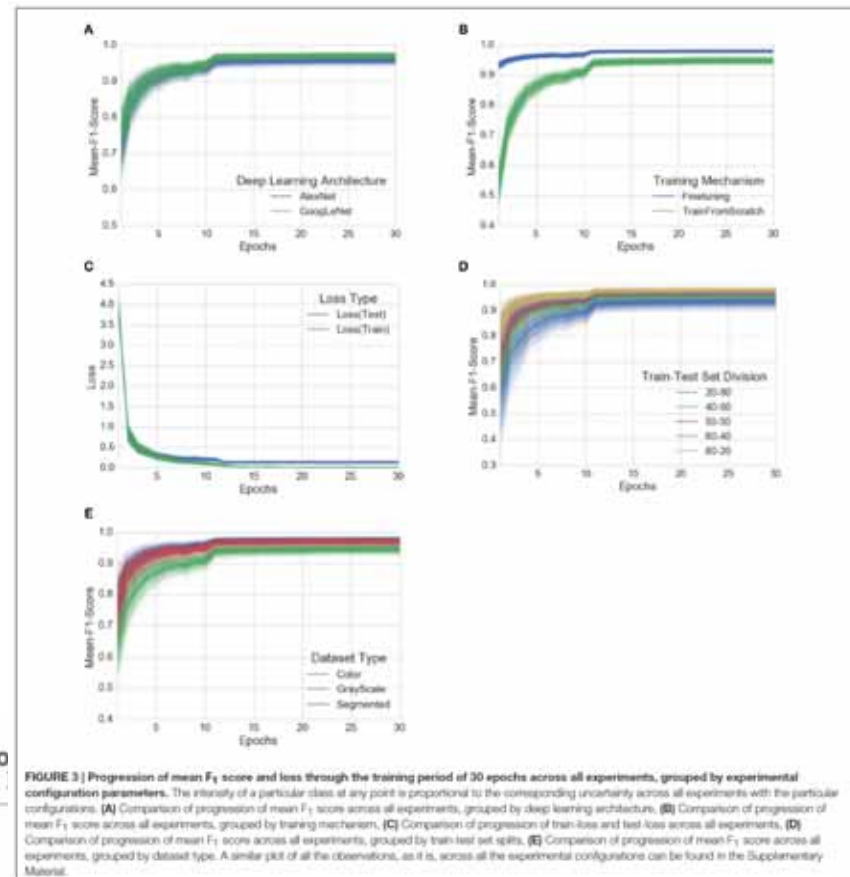


NGRDI (vigor index)

The approach of training **deep learning models** on increasingly large and publicly available image datasets presents a clear path toward smartphone-assisted crop disease diagnosis on a massive global scale.



FIGURE 1 | Example of leaf images from the PlantVillage dataset, representing every crop-disease pair used. (1) Apple Scab, *Venturia inaequalis* (2) Apple Black Rot, *Botryosphaeria obtusa* (3) Apple Cedar Rust, *Gymnosporangium juniperi-virginianae* (4) Apple healthy (5) Blueberry healthy (6) Cherry healthy (7) Cherry Powdery Mildew, *Podosphaera clandestina* (8) Corn Gray Leaf Spot, *Cercospora zeae-maydis* (9) Corn Common Rust, *Puccinia sorghi* (10) Corn healthy (11) Corn Northern Leaf Blight, *Exserohilum turcicum* (12) Grape Black Rot, *Gugrardiea bidwellii*, (13) Grape Black Measles (Esca), *Phaeomoniliella aleophilum*, *Phaeomoniliella chlamydozona* (14) Grape Healthy (15) Grape Leaf Blight, *Pseudocercospora vitis* (16) Orange Huanglongbing (Citrus Greening), *Candidatus Liberibacter* spp. (17) Peach Bacterial Spot, *Xanthomonas campestris* (18) Peach healthy (19) Bell Pepper Bacterial Spot, *Xanthomonas campestris* (20) Bell Pepper healthy (21) Potato Early Blight, *Alternaria solani* (22) Potato healthy (23) Potato Late Blight, *Phytophthora infestans* (24) Raspberry healthy (25) Soybean healthy (26) Squash Powdery Mildew, *Erysiphe cichoracearum* (27) Strawberry Healthy (28) Strawberry Leaf Scorch, *Diplocarpon earlianum* (29) Tomato Bacterial Spot, *Xanthomonas campestris* pv. *vesicatoria* (30) Tomato Early Blight, *Alternaria solani* (31) Tomato Late Blight, *Phytophthora infestans* (32) Tomato Leaf Mold, *Passalora fulva* (33) Tomato Septoria Leaf Spot, *Septoria lycopersici* (34) Tomato Two Spotted Spider Mite, *Tetranychus urticae* (35) Tomato Target Spot, *Corynespora cassiicola* (36) Tomato Mosaic Virus (37) Tomato Yellow Leaf Curl Virus (38) Tomato healthy.



Using Deep Learning for Image-Based Plant Disease Detection

Sharada P. Mohanty^{1,2,3}, David P. Hughes^{4,5,6} and Marcel Salathé^{1,2,3*}

Outline

Affordable Phenotyping

- Sensors
- Platforms
- Environmental characterization
- Data curation and processing
- **Data integration**

Data Integration

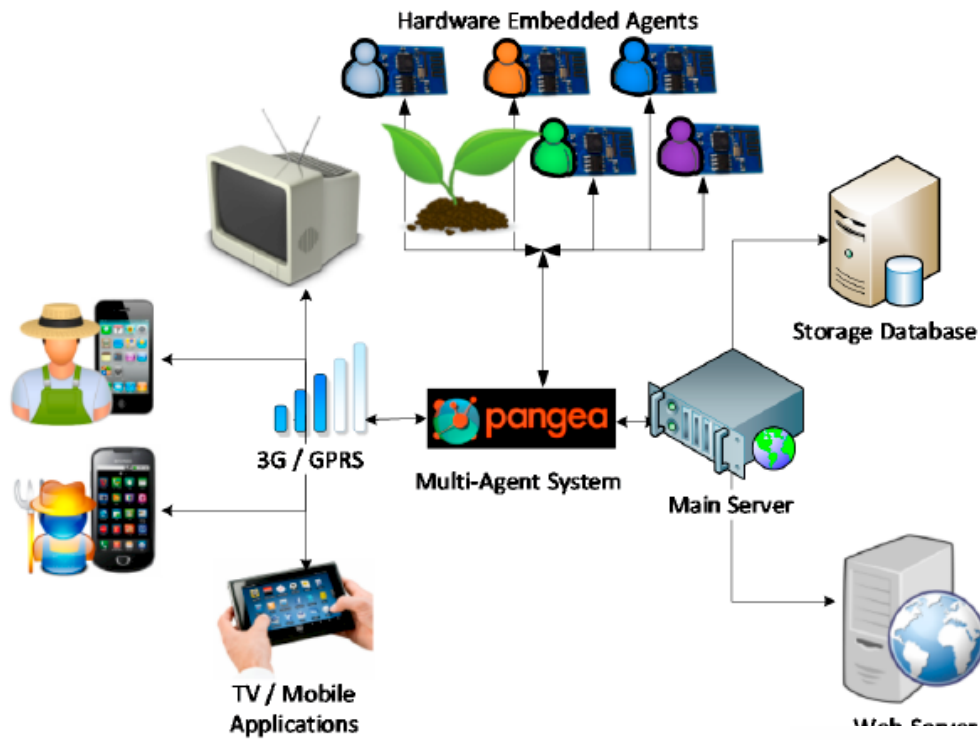


Figure 16. Scheme platform.

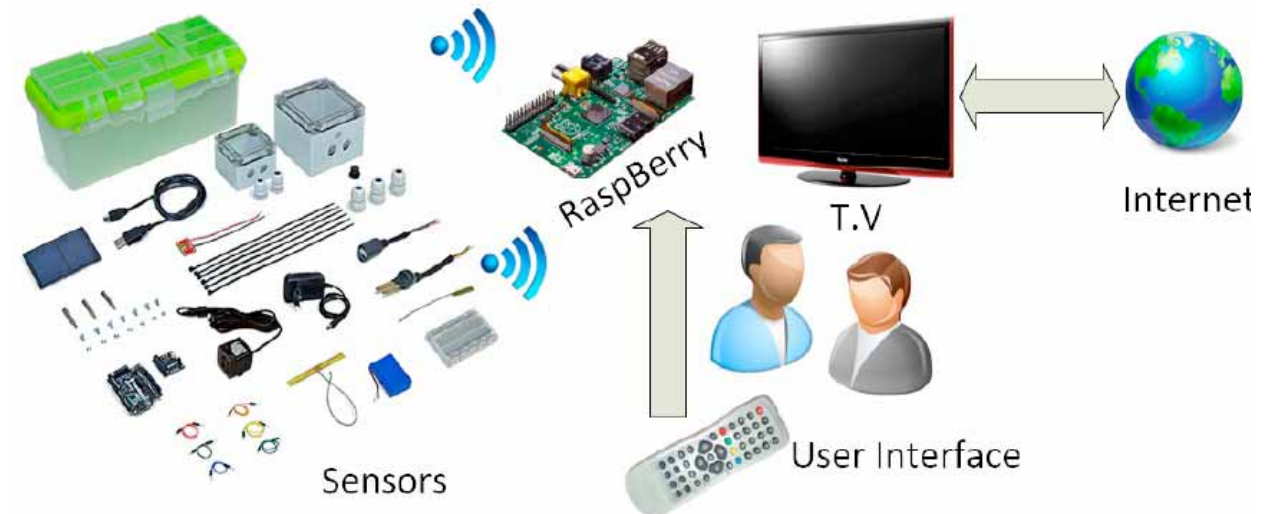
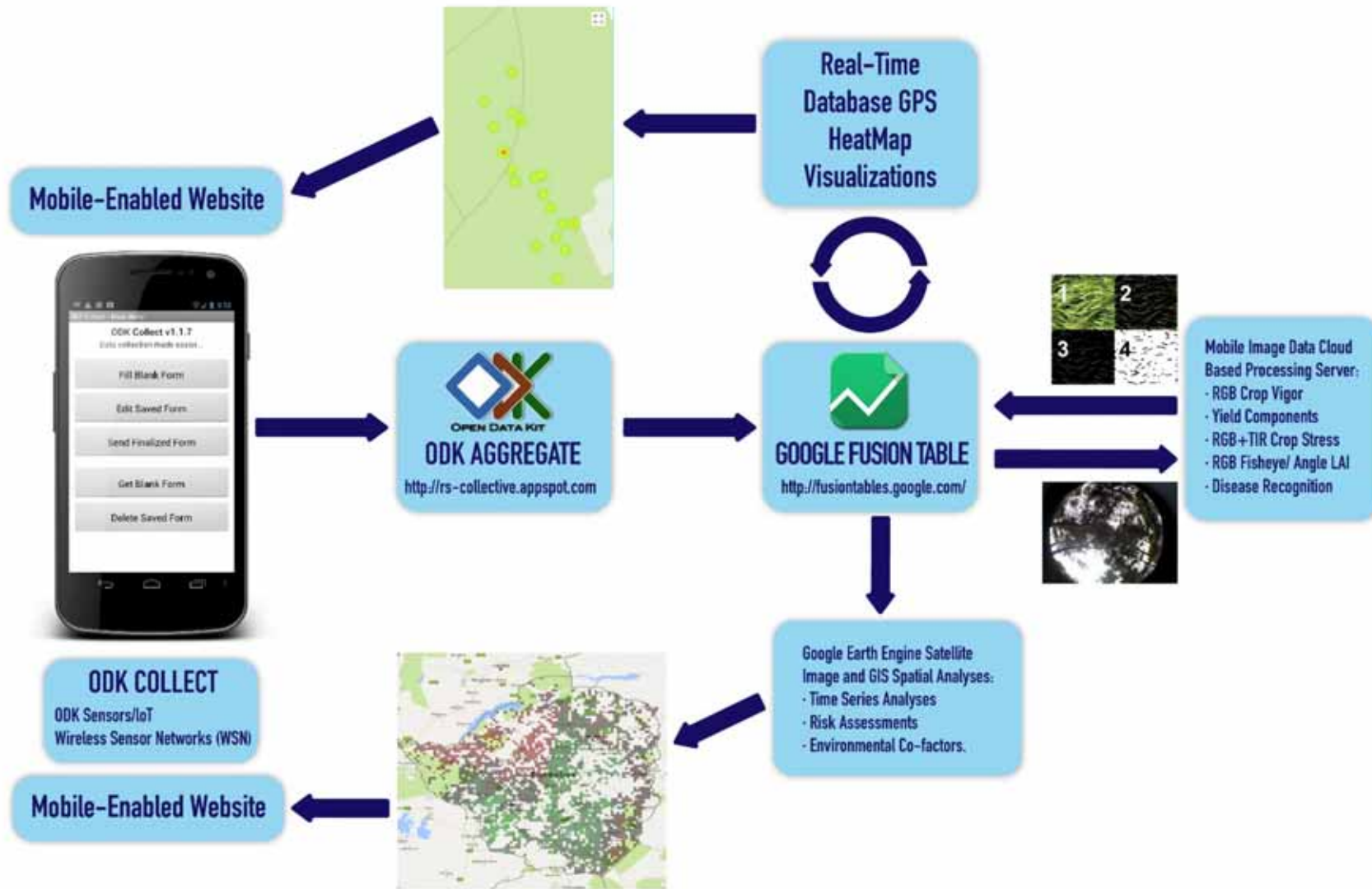
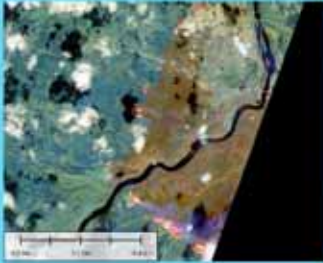


Figure 18. Remote control platform of the irrigation system.

Data integration



EARTH ENGINE



LANDSAT AND SENTINEL
Raw, TOA, SR,....



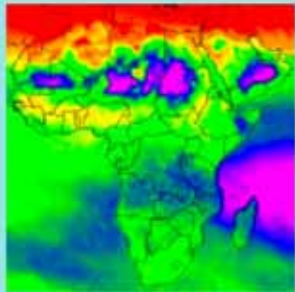
MODIS
Daily, NBAR, LST,....



TERRAIN
SRTM, GTOPO, NED,....



LAND COVER
GlobCover, NLCD,....



Atmospheric Data



Weather



Climate

CLIMATE AND WEATHER



DEMOGRAPHIC
WorldPop/Disease

Conclusions

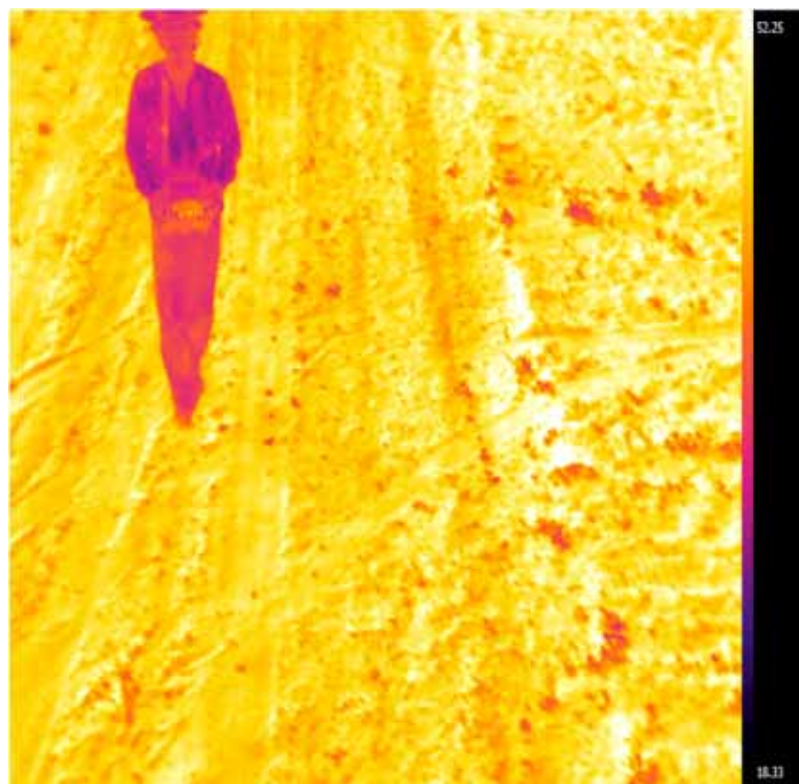
An aerial photograph of a vast agricultural field, likely a cornfield, showing distinct rows of crops. The field is divided into several large rectangular sections by dirt roads or furrows. The crops are a vibrant green color, and the overall scene is captured from a high angle, providing a clear view of the field's layout and the spacing between rows.

Affordable alternatives exist for all the phenotyping components

Acknowledgements



AGL2016-76527-R



Shawn C. Kefauver
Omar Vergara
José A. Fernández
Adrian Gracia
Jordi Bort
Maria D. Serret

Jill Cairns
M. Zaman-Allah
B.M. Prasanna

- University of Barcelona, Faculty of Biology, Integrative Crop Ecophysiology Group
- <http://integrativecropecophysiology.com>,

An aerial photograph of a vast, brown, tilled agricultural field. The field is divided into numerous parallel rows of furrows. In the lower portion of the image, a group of approximately 20-30 people, including men and women in various colorful clothing and head coverings, are scattered across the field, appearing to be engaged in manual labor or inspection. The background shows a flat, green landscape under a clear sky.

Many thanks

Grazie mille

"Shovelomics"

Root crown evaluation

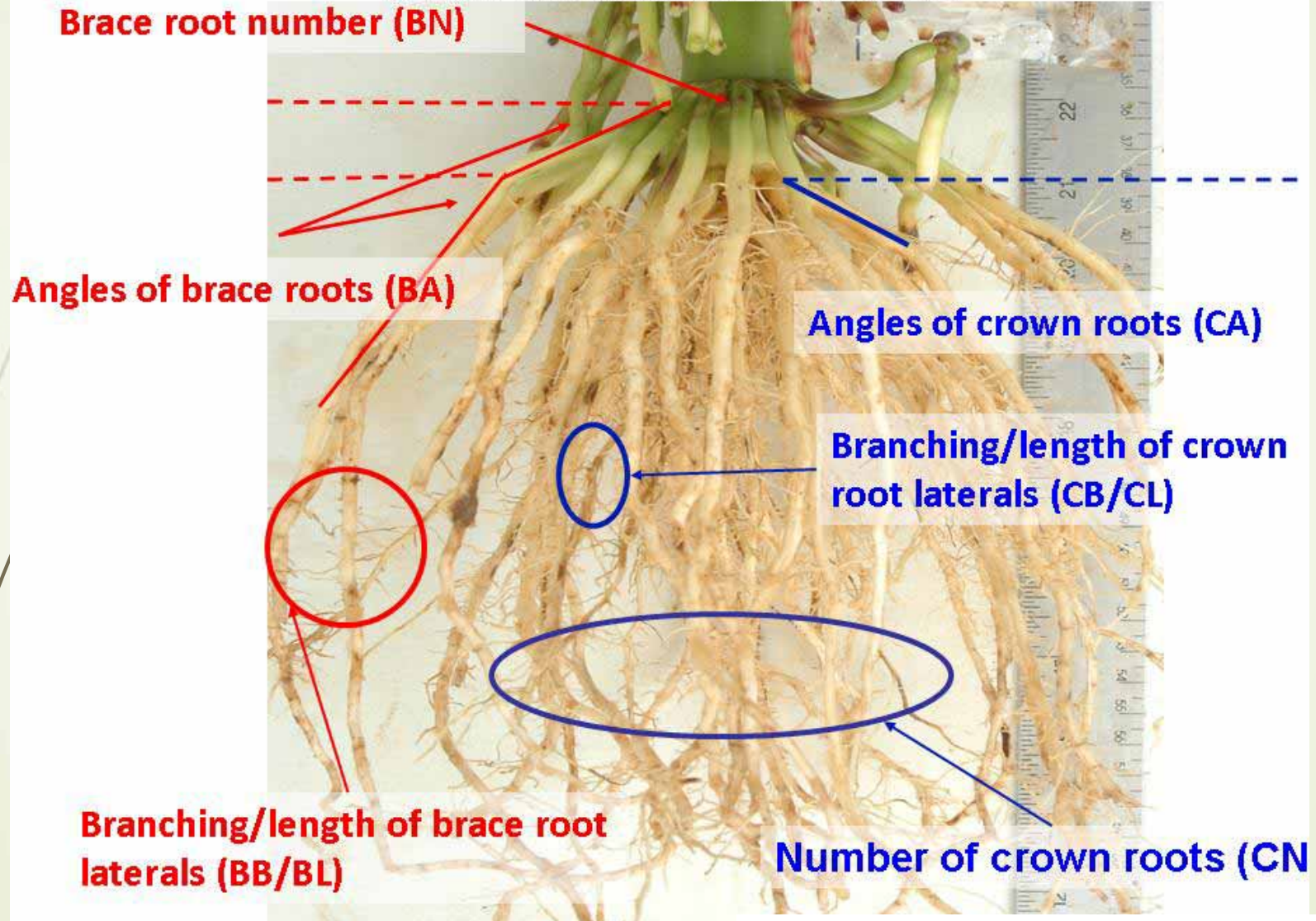


Figure 1. A, Classic shovelomics scoring board to score the angle of maize roots with the soil tissue. B, An example to score rooting depth and angle in common bean.

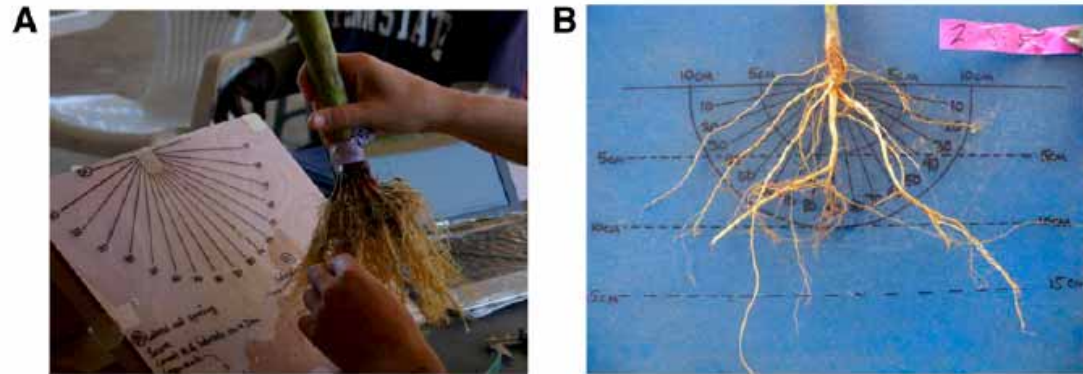
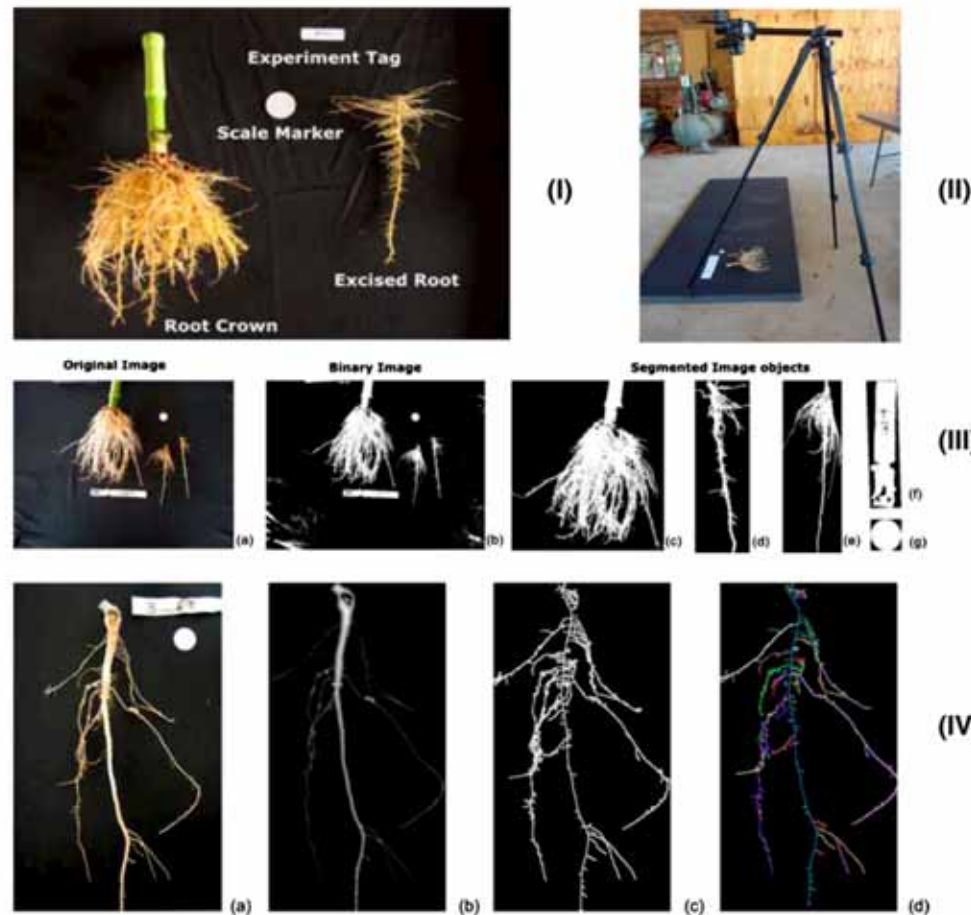


Figure 2. I, Imaging board on the example of a maize root. The experiment tag is used to capture an experiment number, and the scale marker allows the correction of camera tilting and transforming image coordinates into metric units. II, Camera mounted on a tripod placed on top of the imaging board coated with black-board paint. Note that images were taken with protection against direct sunlight not shown in the image. III, Example of the segmentation of the original image into a binary image and then into a series of image masks that serve as input to estimate traits for monocot and dicot roots. The sample is that of a maize root, 40 d after planting at the URBC. IV, The imaging pipeline for dicot roots and sparse monocot roots: Original image on the imaging board (a), derived distance map where the lighter gray level represents a larger diameter of the imaged object (b), medial axis includes loops (c), and loop RTP with a sample of the root branching structure (d). Colors are randomly assigned to each path. The sample is that of a cowpea root, approximately 30 d after planting at the URBC.



Applications and limitations of sensors

Table 2. Applications and limitations of common sensors mounted on field buggies.

Sensor Type	Applications	Limitations
RGB Cameras	Imaging canopy cover and canopy colour. Colour information can be used for deriving information about chlorophyll concentration through greenness indices. The use of 3D stereo reconstruction from multiple cameras or viewpoints allows the estimation of canopy architecture parameters.	No spectral calibration, only relative measurements. Shadows and changes in ambient light conditions can result in under- or over-exposure and limit automation of image processing.
LiDAR and time of flight sensors	Canopy height and canopy architecture in the case of imaging sensors (e.g., LiDAR). Estimation of LAI, volume and biomass. Reflectance from the laser can be used for retrieving spectral information (reflectance in that wavelength).	Integration/synchronization with GPS and wheel encoder position systems is required for georeferencing.
Spectral sensors	Biochemical composition of the leaf/canopy. Pigment concentration, water content, indirect measurement of biotic/abiotic stress. Canopy architecture/LAI with NDVI.	Sensor calibration required. Changes in ambient light conditions influence signal and necessitate frequent white reference calibration. Canopy structure and camera/sun geometries influence signal. Data management is challenging.
Fluorescence	Photosynthetic status, indirect measurement of biotic/abiotic stress.	Difficult to measure in the field at the canopy scale, because of the small signal-to-noise ratio, though laser-induced fluorescence transients (LIFT) can extend the range available, while solar-induced fluorescence can be used remotely.
Thermal sensors	Stomatal conductance. Water stress induced by biotic or abiotic factors.	Changes in ambient conditions lead to changes in canopy temperature, making a comparison through time difficult, necessitating the use of references. Difficult to separate soil temperature from plant temperature in sparse canopies, limiting the automation of image processing. Sensor calibration and atmospheric correction are often required.
Other sensors: electromagnetic induction (EMI), ground penetrating radar (GPR) and electrical resistance tomography (ERT)	Mapping of soil physical properties, such as water content, electric conductivity or root mapping.	Data interpretation is challenging, as heterogeneous soil properties can strongly influence the signal.